THE NATURAL AND PERTURBED OZONOSPHERE

by

Guy BRASSEUR
Anne DE RUDDER
Alain ROUCOUR

Institut d'Aéronomie Spatiale de Belgique
3, Avenue Circulaire, B-1180 Brussels - Belgium.

1. INTRODUCTION

Ozone is of great importance to the human environment. Although the amount of this constituent relatively to the total atmospheric gas is only of the order of 5×10^{-7}, it strongly absorbs solar ultraviolet radiation which would have biologically harmful effects if it penetrated to the Earth's surface. Moreover, this absorption leads to a considerable heating of the upper stratosphere and affects therefore the atmospheric thermal structure and the general circulation.

In recent years, a number of hypotheses have been put forward to show that the injection of various antropogenic gases could lead to a depletion of the ozone amount. Nitrogen oxides injected in the stratosphere by high altitude aircraft have been considered by Johnston (1971) and Crutzen (1970; 1972) to be a real threat to the ozone layer. The release of NO by thermonuclear explosions (Foley and Ruderman, 1972; 1973; Goldsmith et al, 1973; Johnston et al, 1973; Bauer and Gilmore, 1975; Brasseur, 1978) and nitrogen fertilizers (Crutzen, 1974; Mc Elroy et al, 1976) with the possible impact on the ozonosphere has also been considered.

More recently, Molina and Rowland (1974) have predicted large ozone depletion in relation with the injection chlorofluorocarbons produced in large amount by the industry. The seriousness of this problem arises from the rapid increase of the CFC production and from the long time scales for the effects to be seen.

Most analyses of the aeronomical and meteorological mechanisms are based on mathematical computer models which have become essential diagnostic and prognostic tools. These models solve a large number of continuity equations representing the chemical and photochemical reactions as well as the effect of the motions which are responsible for the transport of the long-lived species. In the most sophisticated models, the momentum and the energy conservation equations are also solved in order to make the atmospheric energetics consistent with the chemistry and the photochemistry.

These questions have been widely discussed by the international scientific community and official reports have been published by several national or international agencies. The purpose of this paper is only to review the main processes involved in the ozone problem and to the present some model results, in particular the distribution of several constituents and the predictions of the likely effects of anthropogenic gases.

2. CHEMICAL AND PHOTOCHEMICAL PROCESSES IN THE STRATOSPHERE

The purpose of this section is not to undertake a complete analysis of the aeronomical processes in the stratosphere but to point out the chemical and photochemical reactions which are essential to carry out a quantitative treatment of the ozone chemistry. Further details can be found in review papers which have been recently published (see e.g. Nicolet, 1975; Logan et al., 1978; Johnston and Podolske, 1978).

The balance of the various atmospheric species can be established by writing for the concentration n_i of each constituent i a continuity equation

$$\frac{\partial n_i}{\partial t} + \text{div}\, \vec{\phi}_i = P_i - L_i \qquad (1)$$

where $\vec{\phi}_i$ is the particle flux, P_i and L_i are respectively the local rate of formation and of destruction. The particle flux has to be derived from the momentum and the energy balance equations.

The first photochemical theory of ozone was presented in Paris in 1929 by Chapman and published in 1930. This theory was able to explain the presence of an ozone layer in the middle stratosphere. Twenty years later, it was pointed out by Bates and Nicolet (1950) that the effect of hydrogen radicals was of major importance in the mesosphere and in the upper stratosphere. The possibility of an ozone depletion by nitrogen oxides was suggested in 1970 by Crutzen (1970) and, since the publication of the famous paper by Johnston (1971), special attention has been given to the action of anthropogenic NO_x released in the atmosphere by stratospheric aircraft. Also the effects of nitrate fertilizers, of PCA events and of cosmic rays on the ozonosphere have been considered. More recently Stolarski and Cicerone (1974) suggested that chlorine might constitute an important sink for stratospheric ozone and Molina and Rowland (1974) showed that chlorine could be present in the atmosphere in relatively large amounts due to the industrial release of chlorofluoromethanes at ground level.

These brief considerations show the necessity of treating the stratosphere as a complex interacting chemical system. However, for clarity of presentation, the various reactions will be considered in progression and different steps introduced.

2.1. Ozone in a pure oxygen atmosphere

Ozone is produced essentially between the altitudes of 25 and 60 km. In this atmospheric region, a large number of oxygen molecules are dissociated by U.V. radiation below 242.4 nm. The oxygen atoms produced in this way react rapidly with molecular oxygen to form ozone

$$(J_{O_2}) \; ; \quad O_2 + h\nu \rightarrow O + O$$

$$(k_2) \; ; \quad O + O_2 + M \rightarrow O_3 + M$$

where M is a third body (M = N_2 or O_2 essentially).

The instantaneous production rate of ozone $P(O_3) = 2\, J_{O_2}\, n(O_2)$ varies with altitude, solar zenith angle and ozone content. Integration over the whole atmosphere leads to an ozone production of the order of 10^{17} g/yr. Additional sources are believed to be very small except in the troposphere and in the lower stratosphere where "smog" reactions based on nitrogen oxides and methane are important. The strength of this latter source will appear later in this section.

Ozone is weakly photolyzed to produce stable triplet oxygen atoms $O(^3P)$ by visible light (450 - 650 nm) and by UV radiation of wavelength greater than 310 nm

$$(J_{O_3}) \; ; \quad O_3 + h\nu \rightarrow O(^3P) + O_2$$

Below 310 nm, the photodissociation leads to $O(^1D)$ atoms :

$$(J_{O_3}^{*}) \; ; \quad O_3 + h\nu \rightarrow O(^1D) + O_2$$

The majority of these electronically excited oxygen atoms are deactivated by atmospheric molecules to form $O(^3P)$ but a small fraction of them react with nitrous oxide, water vapor, methane, molecular hydrogen, etc... as it will be seen in the following sections.

Most of the ground state oxygen atoms react with O_2 by reaction (k_2) to reform ozone but a small fraction of them recombine with ozone

$$(k_3)\ ; \quad O + O_3 \rightarrow O_2 + O_2$$

so that the loss rate of ozone in a pure oxygen atmosphere can be written $L(O_3) = 2k_3\ n(O)\ n(O_3)$.

This simple description, represented in fig. 1 is called the Chapman theory of ozone. One can easily show that the corresponding equilibrium time scale of O_3 is less than 1 day at 45 km and larger than 1 year below 25 km. Thus the behavior of ozone will largely differ with altitude : photochemical equilibrium conditions may be assumed in the upper stratosphere but a wide departure occurs in the lower stratosphere, where transport phenomena predominate.

The kinetic equations for atomic oxygen $O(^3P)$ and for ozone can be written

$$\frac{dn(O)}{dt} + k_2\ n(M)\ n(O_2)\ n(O) + k_3\ n(O_3)\ n(O)$$

$$= 2\ J_{O_2}\ n(O_2) + J_{O_3}\ n(O_3) \qquad (2)$$

$$\frac{dn(O_3)}{dt} + (J_{O_3} + J^*_{O_3})\ n(O_3) + k_3 n(O)\ n(O_3) = k_2\ n(M)\ n(O_2) \qquad (3)$$

Since the lifetime of atomic oxygen in the stratosphere is very short, photochemical equilibrium conditions can be adopted (i.e. $d/dt = 0$) and the following expression is a good approximation

$$\frac{n(O)}{n(O_3)} = \frac{J_{O_3}}{k_2\ n(M)\ n(O_2)} \qquad (4)$$

When photochemical equilibrium conditions are valid (above 25 km), the ozone concentration can be quantitatively derived from expression (5).

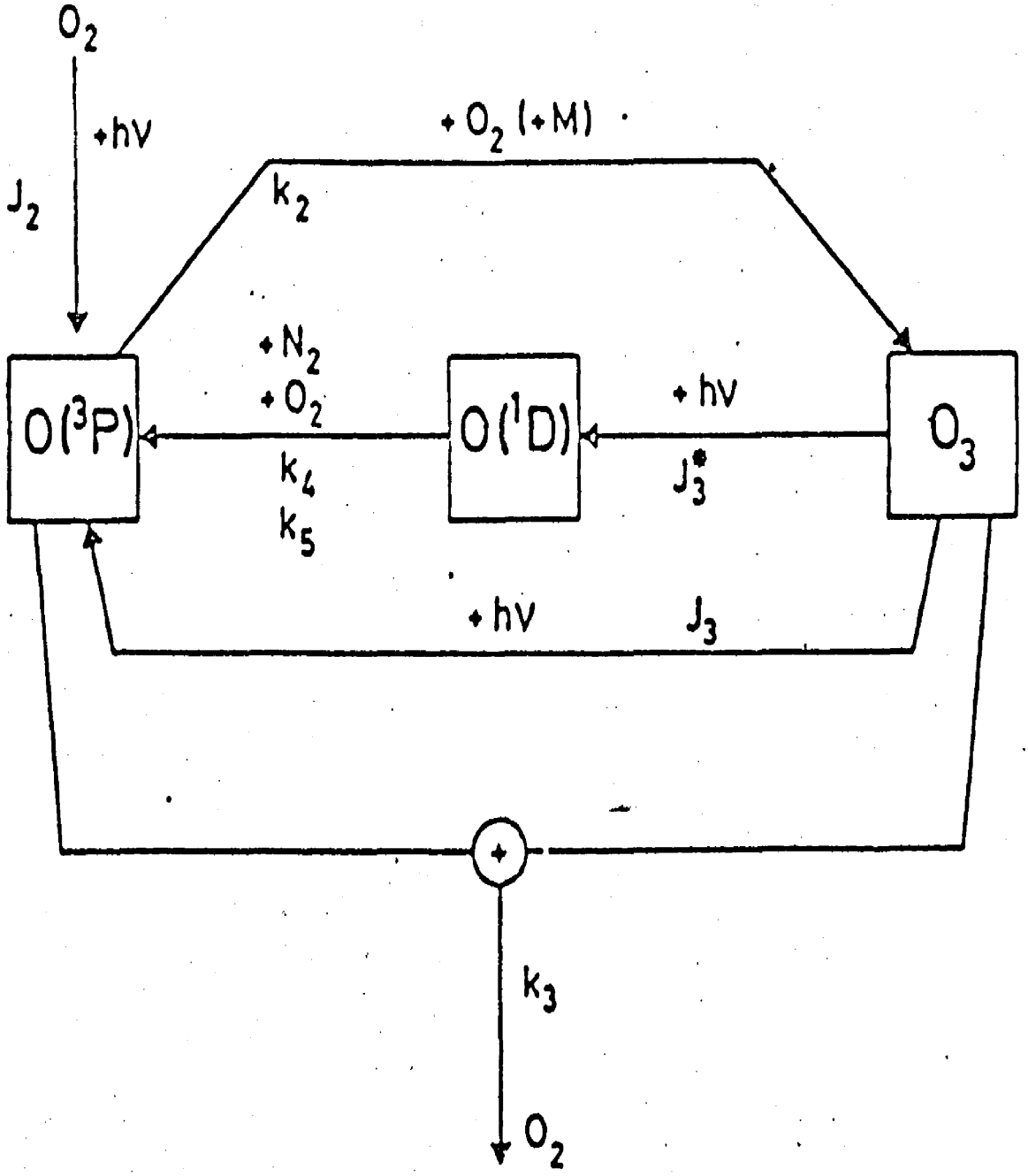

Fig. 1.- Aeronomic reactions in a pure oxygen atmosphere.

$$n^2_{eq}(O_3) = \frac{J_{O_2}}{J_{O_3}} \quad \bar{n}(M)\, n^2(O_2) \quad \frac{k_2}{k_3} \qquad (5)$$

The Chapman theory, and in particular the use of equation (5), leads to a vertical distribution of ozone which does not fit the observations with sufficient precision. In the upper stratosphere and in the mesosphere where photochemical equilibrium conditions may be assumed, the calculated concentration is larger than the reported observations. The discrepancy can be explained by the simplicity of the chemical reaction scheme and different corrections have to be introduced.

2.2. The effect of hydrogen compounds

The first correction may be attributed to the hydrogenated free radicals. The reaction of $O(^1D)$ atoms with water vapor, methane and molecular hydrogen

(a_1^*); $O(^1D) + H_2O \rightarrow OH + OH$

(a_2^*); $O(^1D) + CH_4 \rightarrow CH_3 + OH$

(a_3^*); $O(^1D) + H_2 \rightarrow OH + H$

leads to the formation of hydroxyl radicals and of hydrogen atoms and, after subsequent reaction via

(a_1) ; $H + O_2 + M \rightarrow HO_2 + M$,

to hydroperoxyl radicals.

The following reactions

(a_2) ; $H + O_3 \rightarrow OH + O_2$

(a_6) ; $OH + O_3 \rightarrow HO_2 + O_2$

(a_{6b}) ; $HO_2 + O_3 \rightarrow OH + 2O_2$

(a_5) ; $OH + O \rightarrow H + O_2$

(a_7) ; $HO_2 + O \rightarrow OH + O_2$

constitute destruction mechanisms of odd oxygen with a rate

$$L_{HO_x}(O_3) = [a_2\, n(H) + a_6\, n(OH) + a_{6b}\, n(HO_2)]\, n(O_3) + [a_5\, n(OH) + a_7\, n(HO_2)]\, n(O) .$$

These chemical reactions of HO_x are coupled also by conversion processes which introduce the action of NO and CO :

(a_{26}) ; $HO_2 + NO \rightarrow NO_2 + OH$

(a_{36}) ; $OH + CO \rightarrow CO_2 + H.$

In a more detailed analysis, other molecules such as HNO_3, HO_2NO_2, H_2O_2, CH_4, HOCl have to be considered. Figure 2 shows a schematic representation of the HO_x reaction scheme in the stratosphere.

Since hydroxyl and hyroperoxyl radicals have a very short lifetime in the atmosphere, equilibrium conditions can usually be adopted. Therefore, neglecting the slowest reactions, the steady state equations for H and HO_2 give the ratio of HO_2 to OH as

$$\frac{n(HO_2)}{n(OH)} = \frac{a_5\, n(O) + a_{36}\, n(CO)}{a_7\, n(O) + a_{26}\, n(NO) + a_{6b}\, n(O_3)} \left[\frac{a_1\, n(M)\, n(O_2)}{a_1\, n(M)\, n(O_2) + a_2\, n(O_3)} + \frac{a_6\, n(O_3)}{a_5\, n(O) + a_{36}\, n(CO)} \right] \qquad (6)$$

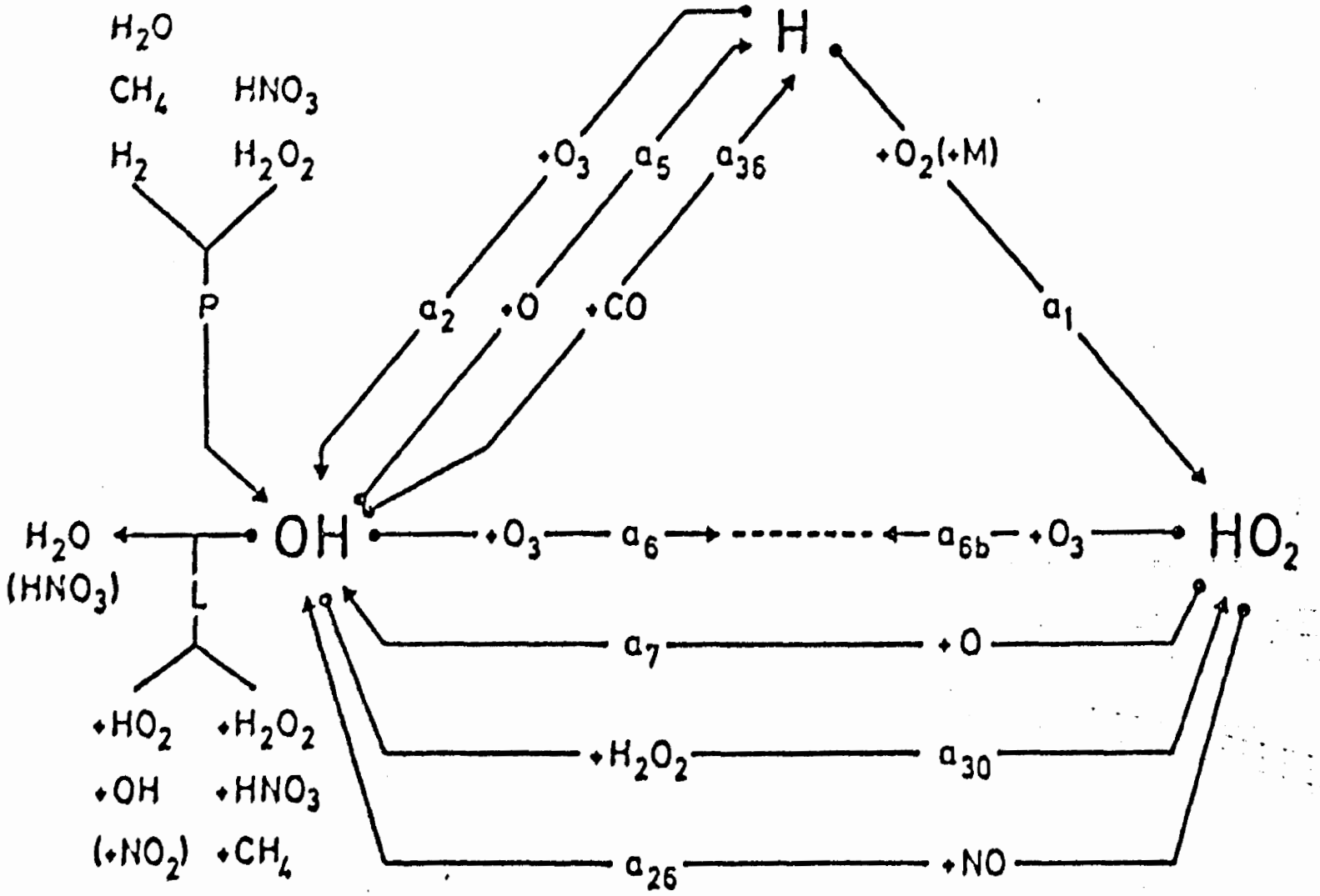

Fig. 2.- Main chemical reactions in the stratosphere related to the hydroxyl radicals.

Near the stratopause, a good approximation to expression (6) is

$$\frac{n(HO_2)}{n(OH)} \simeq \frac{a_5}{a_7} \simeq 1$$

while, in the lower stratosphre, one may write

$$\frac{n(HO_2)}{n(OH)} = \frac{a_6\, n(O_3) + a_{36}\, n(CO)}{a_{6b}\, n(O_3) + a_{26}\, n(NO)} .$$

The most important destruction reaction for HO_x in the middle and upper stratosphere is the recombination of OH and HO_2

$$(a_{17}) \; ; \; OH + HO_2 \rightarrow H_2O + O_2$$

In the lower stratosphere and in the troposphere, the main destruction is due to the following reactions :

$$OH + HNO_3 \rightarrow H_2O + NO_3$$

$$OH + HO_2NO_2 \rightarrow H_2O + NO_2 + O_2$$

$$OH + H_2O_2 \rightarrow H_2O + HO_2$$

Moreover the reaction

$$(c_2) \; ; \; CH_4 + OH \rightarrow CH_3 + H_2O$$

has to be taken into account and the global balance of hydroxyl and hydroperoxyl radicals can be written in a simple form by the following equation (see Nicolet, 1975)

$$n(O(^1D))\, [a_1^* \, n(H_2O) + a_2^* \left(\frac{1+X}{2} \right) n(CH_4) + a_3^* \, n(H_2)] = a_{17}\, n(OH)\, n(HO_2)$$

$$+ c_2 \left(\frac{1-X}{2} \right) n(CH_4)\, n(OH) \qquad (7)$$

where X is a function related to the branching ratio of the photodissociation rate of formaldehyde (Nicolet, 1975); its value is in the range of 1-2.

2.3. The effect of nitrogen oxides

The second correction which has to be applied to the Chapman theory is the effect of nitrogen oxides. The main source of nitric oxide NO is due to the oxidation of nitroux oxide N_2O. This latter constituent is produced at ground level by anaerobic bacterial processes. It is transported into the stratosphere where it is photodissociated

$$(J_{N_2O}) \; ; \; N_2O + h\nu \rightarrow N_2 + O(^1D)$$

or destroyed by oxidation :

$$(b_{38}) \; ; \; N_2O + O(^1D) \rightarrow N_2 + O_2$$

$$(b_{39}) \; ; \; N_2O + O(^1D) \rightarrow 2NO$$

The continuity equation for nitrous oxide is thus

$$\frac{\partial n(N_2O)}{\partial t} + \text{div}\, \vec{\phi}\,(N_2O) + [J_{N_2O} + (b_{38} + b_{39})\, n(O(^1D))]\, n(N_2O) = 0 \qquad (8)$$

and the production rate of NO is

$$P(NO) = 2b_{39}\, n(O(^1D))\, n(N_2O).$$

As mentioned above, additional sources of nitric oxide can be considered : the dissociative ionization of N_2 by cosmic rays (see Brasseur and Nicolet, 1973; Nicolet, 1974) or the effect of PCA events (see Crutzen et al., 1975).

Nitric oxide is converted into nitrogen dioxide by reactions

(b_4) ; $NO + O_3 \rightarrow NO_2 + O_2$

(a_{26}) ; $NO + HO_2 \rightarrow NO_2 + OH$

(c_5) ; $NO + CH_3O_2 \rightarrow NO_2 + CH_3O$

but NO_2 is quickly reconverted into NO during the day by the following processes :

(J_{NO_2}) ; $NO_2 + h\nu \rightarrow NO + O$

(b_3) ; $NO_2 + O \rightarrow NO + O_2$

The ratio of the NO to NO_2 concentration is thus given by

$$\frac{n(NO)}{n(NO_2)} = \frac{J_{NO_2} + b_3\, n(O)}{b_4\, n(O_3) + a_{26}\, n(HO_2) + c_5\, n(CH_3O_2)} \qquad (9)$$

It can be easily seen that reactions (b_4) and (b_3) constitute a catalytical cycle destroying odd oxygen. Considering that the photodissociation of NO_2 leads to the formation of $O(^3P)$ which is quickly transformed by reaction (k_2) into ozone, the additional source term of O_3 related to nitrogen oxide becomes

$$P_{NO_x}(O_3) - L_{NO_x}(O_3) = J_{NO_2}\, n(NO_2) - b_4\, n(NO)\, n(O_3) - b_3\, n(NO_2)\, n(O)$$

or, if expression (9) is used,

$$P_{NO_x}(O_3) - L_{NO_x}(O_3) = [a_{26}\, n(HO_2) + c_5\, n(CH_3O_2)]\, n(NO) - 2b_3\, n(NO_2\, n(O)$$

Thus, it appears that the action of nitrogen oxides on ozone is characterized by an additional loss term in the middle and upper stratosphere and a production term in the lower stratosphere and in the tropo-

sphere, as shown in fig. 3. In the simple model which has been used for the computation of $P_{NO_x}(O_3)$ and $L_{NO_x}(O_3)$, the cross-over point appears to be at the altitude of 13 km. Thus the ozone production due to nitrogen oxides which is of great importance to understanding the ozone budget, requires a precise determination of the HO_2 and CH_3O_2 concentrations.

Other reactions have to be considered since they convert NO and NO_2 into other molecules which have no direct chemical effect on ozone and thus constitute reservoirs for nitrogen oxides. These molecules are for example NO_3, N_2O_5, HNO_3, HO_2NO_2, etc... The most important processes are

- formation and destruction of HNO_3

(b_{22}) ; $NO_2 + OH + M \rightarrow HNO_3 + M$
(J_{HNO}) ; $HNO_3 + h\nu \rightarrow NO_2 + OH$
(b_{27}) ; $HNO_3 + OH \rightarrow NO_3 + H_2O$

- formation and destruction of NO_3

(b_9) ; $NO_2 + O_3 \rightarrow NO_3 + O_2$
$J^1_{NO_3}$; $NO_3 + h\nu \rightarrow NO + O_2$
$J^2_{NO_3}$; $NO_3 + h\nu \rightarrow NO_2 + O$

- formation and destruction of N_2O_5

(b_{12}) ; $NO_3 + NO_2 + M \rightarrow N_2O_5 + M$
$(J_{N_2O_5})$; $N_2O_5 + h\nu \rightarrow NO_3 + NO_2$
(b_{32}) ; $N_2O_5 + M \rightarrow NO_3 + NO_2 + M$

- formation and destruction of HO_2NO_2

(b_{23}) ; $NO_2 + HO_2 \rightarrow HO_2NO_2$
$(J_{HO_2NO_2})$; $HO_2NO_2 + h\nu \rightarrow NO_2 + HO_2$

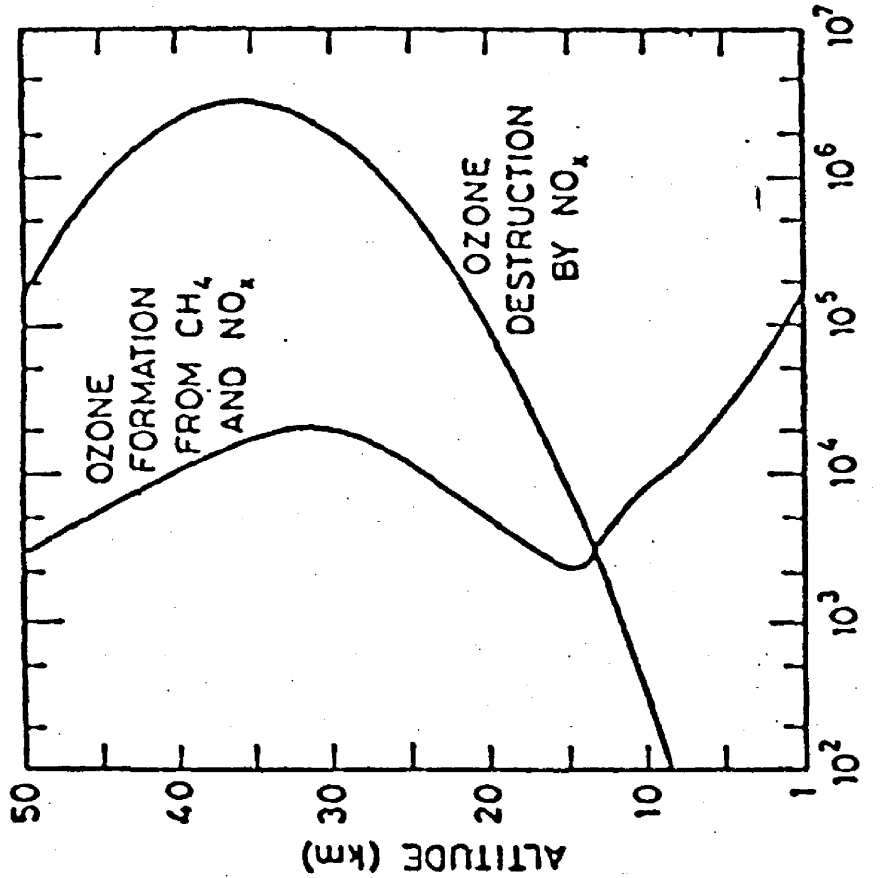

Fig. 3.- Production rate and destruction rate of ozone by nitrogen oxides.

Figure 4 gives a diagram of the principal reactions related to nitrogen oxides in the stratosphere and in the mesosphere (where atomic nitrogen has to be taken into account.

2.4. The effect of chlorinated species.

The third correction to the Chapman theory of ozone is the introduction into the reaction scheme of chlorine and its derivatives. Chlorine atoms are produced by dissociation of halocarbons which are released at ground level and diffuse slowly towards the stratosphere. The main natural source of chlorine seems to be due to methyl chloride CH_3Cl which is photodissociated in the stratosphere

$$(J_{CH_3Cl}) \; ; \qquad CH_3Cl + h\nu \rightarrow CH_3 + Cl$$

or destroyed by OH in the stratosphere and in the troposphere

$$(d_1) \; ; \qquad CH_3Cl + OH \rightarrow CH_2Cl + H_2O \; .$$

The industrial halocarbons which play the major role as anthropogenic sources of chlorine are carbon tetrachloride CCl_4, trichlorofluoromethane $CFCl_3$ (freon 11) and dichlorodifluoromethane CF_2Cl_2 (freon 12). These gases are photolyzed in the stratosphere by UV radiation

$$(J_{CCl_4}) \; ; \qquad CCl_4 + h\nu \rightarrow CCl_3 + Cl$$

$$(J_{CFCl_3}) \; ; \qquad CFCl_3 + h\nu \rightarrow CFCl_2 + Cl$$

$$(J_{CF_2Cl_2}) \; ; \qquad CF_2Cl_2 + h\nu \rightarrow CF_2Cl + Cl$$

The continuity equations for these species are

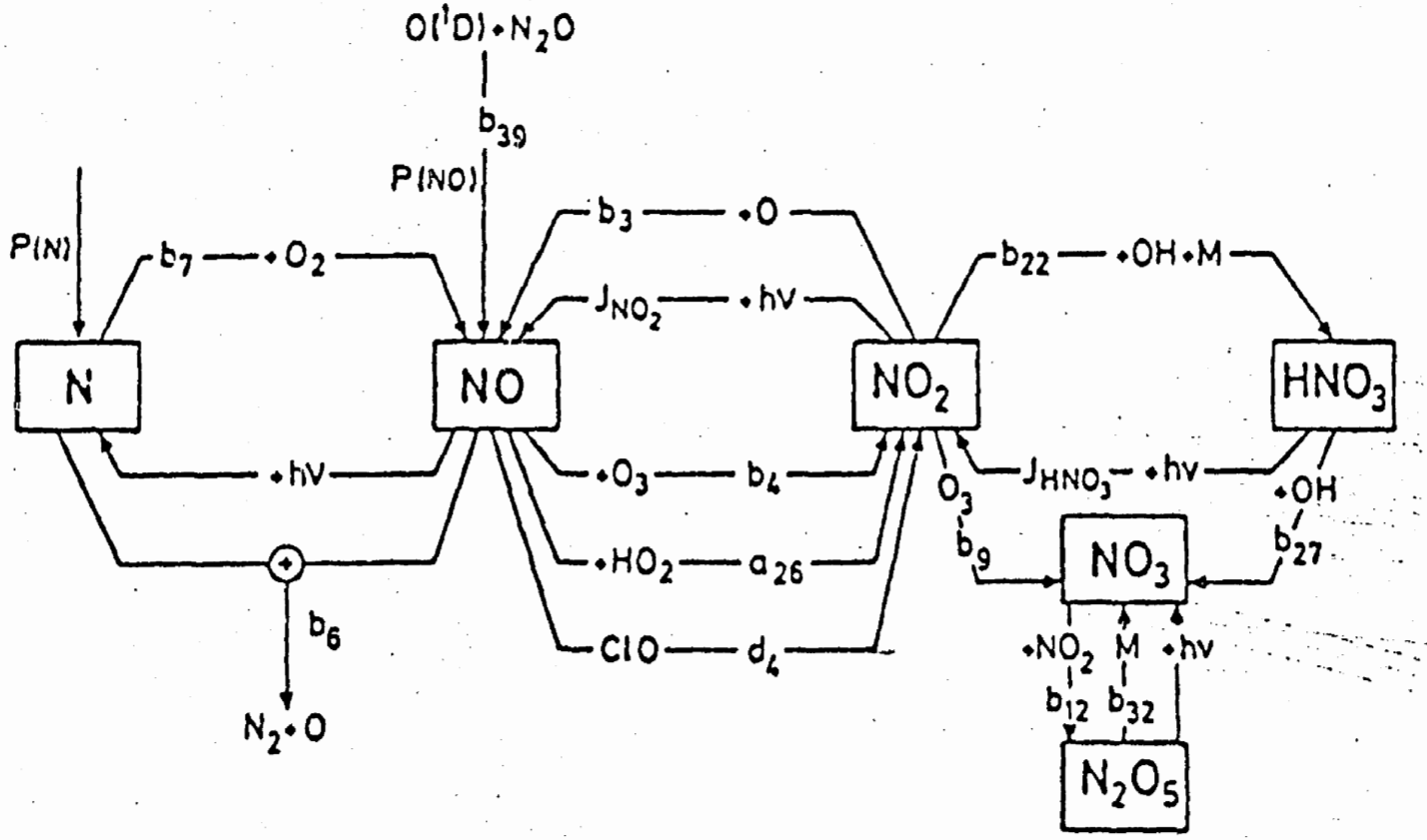

Fig. 4.- Main chemical and photochemical reactions of the nitrogen species in the stratosphere.

$$\frac{\partial n\,(CH_3Cl)}{\partial t} + \text{div}\,\vec{\phi}\,(CH_3Cl) + [J_{CH_3Cl} + d_1\, n(OH)]\, n(CH_3Cl) = 0 \qquad (10)$$

$$\frac{\partial n\,(CCl_4)}{\partial t} + \text{div}\,\vec{\phi}\,(CCl_4) + J_{CCl_4}\, n(CCl_4) = 0 \qquad (11)$$

$$\frac{\partial n\,(CFCl_3)}{\partial t} + \text{div}\,\vec{\phi}\,(CFCl_3) + J_{CFCl_3}\, n(CFCl_3) = 0 \qquad (12)$$

$$\frac{\partial n(CF_2Cl_2)}{\partial t} + \text{div}\,\vec{\phi}\,(CF_2Cl_2) + J_{CF_2Cl_2}\, n(CF_2Cl_2) = 0 \qquad (13)$$

Similar equations can be written for the other halocarbons which are released in the atmosphere. But considering only these four constituents and assuming that they are completely dissociated after subsequent reactions, the production rate of chlorine atoms is given by

$$P(ClX) = 4\, J_{CCl_4}\, n(CCl_4) + 3\, J_{CFCl_3}\, n(CFCl_3) + 2\, J_{CF_2Cl_2}\, n(CF_2Cl_2) + [J_{CH_3Cl} + d_1\, n(OH)]\, n(CH_3Cl)$$

The chlorine atoms react rapidly with ozone to form chlorine monoxide ClO which is reconverted into Cl by atomic oxygen and nitric oxide

$$(d_2)\ ; \quad Cl + O_3 \rightarrow ClO + O_2$$
$$(d_3)\ ; \quad ClO + O \rightarrow Cl + O_2$$
$$(d_4)\ ; \quad ClO + NO \rightarrow Cl + NO_2$$

The coupling of reactions (d_2) and (d_3) constitute a catalytic cycle for the destruction of odd oxygen and the corresponding loss rate for O_x is

$$L_{ClX}\,(O_x) = 2\, d_3\, n(ClO)\, n(O)$$

The ratio of the Cl to the ClO concentration is given by

$$\frac{n(Cl)}{n(ClO)} = \frac{d_3\, n(O) + d_4\, n(NO)}{d_2\, n(O_3)} \qquad (14)$$

Again, other reactions have to be considered since they lead to the formation of molecules such as HCl, $ClONO_2$, HOCl which constitute "reservoirs" for chlorine atoms and chlorine monoxide. The most important processes are

- Formation and destruction of HCl

$$Cl + CH_4 \rightarrow HCl + CH_3$$
$$Cl + HO_2 \rightarrow HCl + O_2$$
$$HCl + h\nu \rightarrow H + Cl$$
$$HCl + OH \rightarrow H_2O + Cl$$

- Formation and destruction of $ClONO_2$

$$ClO + NO_2 + M \rightarrow ClONO_2 + M$$
$$ClONO_2 + h\nu \rightarrow ClO + NO_2$$
$$ClONO_2 + O \rightarrow \text{products}$$

- Formation and destruction of HOCl

$$ClO + HO_2 \rightarrow HOCl + O_2$$
$$HOCl + h\nu \rightarrow Cl + OH$$

The ClX chemistry in the stratosphere is schematically represented on fig. 5. This last equation can be simplified when the relations between NO and NO_2 on the one hand and between Cl and ClO on the other hand are expressed. An approximate but general balance equation for ozone can be written :

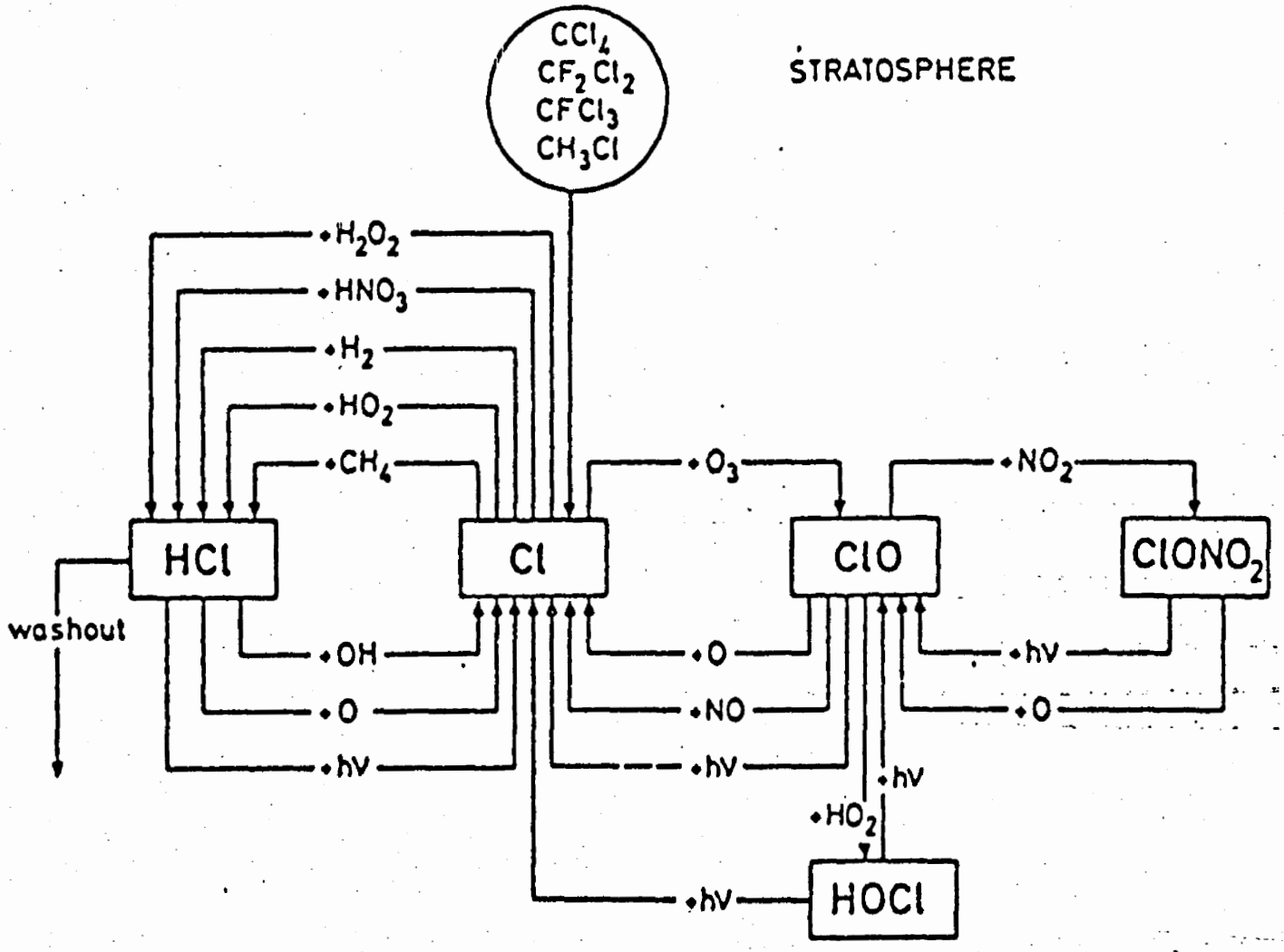

Fig. 5.- Main chemical and photochemical reactions of the chlorine species in the stratosphere.

$$\frac{\partial n\,(O_3)}{\partial t} + \operatorname{div} \vec{\phi}\,(O_3) + 2k_3\, n(O)\, n(O_3)$$

$$+ [a_5\, n(OH) + a_7\, n(HO_2) + 2b_3\, n(NO_2) + 2d_3\, n(ClO)]\, n(O)$$

$$+ [a_2\, n(H) + a_6\, n(OH) + a_{6b}\, n(HO_2)]\, n(O_3)$$

$$= 2\, J_{O_2}\, n(O_2) + [a_{26}\, n(HO_2) + c_5\, n(CH_3O_2)]\, n(NO) \qquad (15)$$

It should be emphasized that the transport term (div $\vec{\phi}(O_3)$) becomes dominant in the regions where the replacement time $\tau = n(O_3)/P(O_3)$ becomes larger than the residence time of inert tracers, roughly two years. Near the equator, the photochemical replacement times are very short compared to stratospheric residence times except near the tropopause, where the times are comparable. At middle and high latitude, the ozone replacement time τ below 20 km are much longer than residence times. In the region where τ is between 4 months and 10 years, the ozone distribution is a complicated function of photochemical formation, air transport and chemical destruction.

The efficiency of a chemical reaction is described by its rate constant which is generally a function of the temperature T. Table 1 gives the presently preferred values of the rate constants characterizing the most important chemical reactions in the ozonosphere. The efficiency of a photochemical reaction is provided by the photodissociation coefficient J of the corresponding molecule X. It is given by the following expression :

$$J\,(X;\, z,\, \chi) = \int_{\lambda} \varepsilon(X;\, \lambda).\, \sigma(X;\, \lambda).\, q(\lambda,\, z,\, \chi).\, d\lambda \qquad (16)$$

where $\sigma(X;\, \lambda)$ is the absorption cross section at wavelength λ, $\varepsilon(X,\, \lambda)$ is the corresponding quantum yield of the photodissociation and $q(\lambda,\, z,\, \chi)$ is the solar irradiance at altitude z and for a zenith angle of the Sun given by χ. The integral has to be performed on all wavelengths which have to be considered for the photodissociation. When penetrating

TABLE 1 : Reaction rates of the most important reactions in the stratosphere (WMO, 1982).

Reactions	Rate constants $cm^3\ s^{-1}$
$O + O + M \rightarrow O_2 + M$	$k_1 = 4.7 \times 10^{-33} \left(\frac{300}{T}\right)^2 n(M)$
$O + O_2 + M \rightarrow O_3 + M$	$k_2 = 6.2 \times 10^{-34} \left(\frac{300}{T}\right)^2 n(M)$
$O + O_3 \rightarrow 2\ O_2$	$k_3 = 1.5 \times 10^{-11}\ e^{-2218/T}$
$O(^1D) + N_2 \rightarrow O(^3P) + N_2$	$k_4 = 1.8 \times 10^{-11}\ e^{107/T}$
$O(^1D) + O_2 \rightarrow O(^3P) + O_2$	$k_5 = 3.2 \times 10^{-11}\ e^{67/T}$
$H + O_2 + M \rightarrow HO_2 + M$	$a_1 = 5.5 \times 10^{-32} \left(\frac{T}{300}\right)^{-1.4} n(M)$
$H + O_3 \rightarrow O_2 + OH_{v \leq 9}$	$a_2 = 1.4 \times 10^{-10}\ e^{-470/T}$
$OH + O \rightarrow H + O_2$	$a_5 = 2.3 \times 10^{-11}\ e^{110/T}$
$OH + O_3 \rightarrow HO_2 + O_2$	$a_6 = 1.6 \times 10^{-12}\ e^{-940/T}$
$HO_2 + O_3 \rightarrow OH + 2O_2$	$a_{6b} = 1.4 \times 10^{-14}\ e^{-580/T}$
$HO_2 + O \rightarrow O_2 + OH_{v \leq 6}$	$a_7 = 3.5 \times 10^{-11}$
$OH + HO_2 \rightarrow H_2O + O_2$	$a_{17} = 8 \times 10^{-11}$
$H + HO_2 \rightarrow OH + OH$	$a_{23a} = 4.2 \times 10^{-10}\ e^{-950/T}$
$H + HO_2 \rightarrow H_2 + O_2$	$a_{23b} = 4.2 \times 10^{-11}\ e^{-350/T}$
$H + HO_2 \rightarrow H_2O + O$	$a_{23c} = 8.3 \times 10^{-11}\ e^{-500/T}$
$HO_2 + NO \rightarrow NO_2 + OH$	$a_{26} = b_{29} = 3.7 \times 10^{-12}\ e^{240/T}$
$HO_2 + HO_2 \rightarrow H_2O_2 + O_2$	$a_{27} = 3.0 \times 10^{-12}$
$OH + CO \rightarrow CO_2 + H$	$a_{36} = 1.35 \times 10^{-13}\ (1 + P_{atm})$
$O(^1D) + H_2O \rightarrow OH + OH$	$a_1^* = 2.3 \times 10^{-10}$
$O(^1D) + CH_4 \rightarrow CH_3 + OH$	$a_2^* = 1.4 \times 10^{-10}$
$O(^1D) + H_2 \rightarrow OH + H$	$a_3^* = 1.0 \times 10^{-10}$
$CH_4 + OH \rightarrow CH_3 + H_2O$	$c_2 = 2.4 \times 10^{-12} e^{-1710/T}$
$CH_3O_2 + NO \rightarrow CH_3O + NO_2$	$c_5 = 7.4 \times 10^{-12}$
$O(^3P) + NO_2 \rightarrow NO + O_2$	$b_3 = 9.3 \times 10^{-12}$
$O_3 + NO \rightarrow NO_2 + O_2$	$b_4 = 3.8 \times 10^{-12}\ e^{-1580/T}$
$N(^4S) + NO \rightarrow N_2 + O$	$b_6 = 3.7 \times 10^{-11}$
$N(^4S) + O_2 \rightarrow NO + O$	$b_7 = 4.0 \times 10^{-12}\ e^{-3220/T}$
$NO_2 + O_3 \rightarrow NO_3 + O_2$	$b_9 = 1.2 \times 10^{-13}\ e^{-2450/T}$

Reactions	Rate constants $cm^3\ s^{-1}$
$NO_3 + NO_2 + M \rightarrow N_2O_5 + M$	b_{12} : see below
$NO_2 + OH + M \rightarrow HNO_3 + M$	b_{22} : see below
$HNO_3 + OH \rightarrow H_2O + NO_3$	$b_{27} = 1.5 \times 10^{-14}\ e^{650/T}$
$N_2O_5 + M \rightarrow NO_3 + NO_2 + M$	$b_{32} = 2.2 \times 10^{-5}\ e^{-9700/T}$
$N_2O + O(^1D) \rightarrow N_2 + O_2$	$b_{38} = 4.4 \times 10^{-11}$
$N_2O + O(^1D) \rightarrow 2NO$	$b_{39} = 7.2 \times 10^{-11}$
$HO_2 + NO_2 + M \rightarrow HO_2NO_2 + M$	b_{23} : see below
$HO_2NO_2 + OH \rightarrow$ products	$b_{30} = 4 \times 10^{-12}$
$CH_3Cl + OH \rightarrow CH_2Cl + H_2O$	$d_1 = 1.8 \times 10^{-12}\ e^{-1112/T}$
$Cl + O_3 \rightarrow ClO + O_2$	$d_2 = 2.8 \times 10^{-11}\ e^{-257/T}$
$ClO + O \rightarrow Cl + O_2$	$d_3 = 7.7 \times 10^{-11}\ e^{-130/T}$
$ClO + NO \rightarrow Cl + NO_2$	$d_4 = 6.2 \times 10^{-12}\ e^{+294/T}$
$Cl + CH_4 \rightarrow HCl + CH_3$	$d_5 = 9.6 \times 10^{-12}\ e^{-1350/T}$
$Cl + HO_2 \rightarrow HCl + O_2$	$d_7 = 4.8 \times 10^{-11}$
$HCl + OH \rightarrow Cl + H_2O$	$d_{11} = 2.8 \times 10^{-12}\ e^{-425/T}$
$ClO + NO_2 + M \rightarrow ClONO_2 + M$	d_{22} : see below
$ClONO_2 + O \rightarrow$ products	$d_{32} = 3.0 \times 10^{-12}\ e^{-808/T}$
$ClO + HO_2 \rightarrow HOCl + O_2$	$d_{35} = 4.6 \times 10^{-13}\ e^{710/T}$
$CH_3CCl_3 + OH \rightarrow CH_2CCl_3 + H_2O$	$d_{50} = 5.4 \times 10^{-12}\ e^{-1820/T}$

Three-body reactions with the following expression for their rate constant k ($cm^3\ s^{-1}$).

$$k = \left[\frac{k_o\ n(M)^-}{1 + k_o\ n(M)/k_\infty} \right] 0.6 \left\{ 1 + [\log_{10} (k_o\ n(M)/k_\infty)]^2 \right\}^{-1}$$

with $k_o = k_o^{300}\ (T/300)^{-n}$

$k_\infty = k_\infty^{300}\ (T/300)^{-m}$

$NO_3 + NO_2 + M \rightarrow N_2O_5 + M$	$k_o^{300} = 1.4 \times 10^{-30}$ $n = 2.8$ $k_\infty^{300} = 8 \times 10^{-13}$ $m = 0$
$NO_2 + OH + M \rightarrow HNO_3 + M$	$k_o^{300} = 2.6 \times 10^{-30}$ $n = 2.9$ $k_\infty^{300} = 2.4 \times 10^{-11}$ $m = 1.3$
$NO_2 + HO_2 + M \rightarrow HO_2NO_2 + M$	$k_o^{300} = 2.1 \times 10^{-31}$ $n = 5$ $k_\infty^{300} = 6.5 \times 10^{-12}$ $m = 2$
$ClO + NO_2 + M \rightarrow ClONO_2 + M$	$k_o^{300} = 4.5 \times 10^{-32}$; 1.2×10^{-31} (isomer) $n = 3.8$ $k_\infty^{300} = 1.5 \times 10^{-11}$ $m = 1.9$

TABLE 2 : Photochemical reactions in the stratosphere.

$O_2 + h\nu \rightarrow O + O$

$O_3 + h\nu \rightarrow O + O_2$

$O_3 + h\nu \rightarrow O(^1D) + O_2$

$NO + h\nu \rightarrow N + O$

$NO_2 + h\nu \rightarrow NO + O$

$NO_3 + h\nu \rightarrow$ products

$N_2O + h\nu \rightarrow N_2 + O(^1D)$

$N_2O_5 + h\nu \rightarrow$ products

$H_2O + h\nu \rightarrow H + OH$

$H_2O_2 + h\nu \rightarrow Oh + OH$

$HNO_3 + h\nu \rightarrow OH + NO_2$

$HNO_4 + h\nu \rightarrow$ products

$CO_2 + h\nu \rightarrow CO + O$

$CH_4 + h\nu \rightarrow$ products

$ClO + h\nu \rightarrow Cl + O$

$HCl + h\nu \rightarrow H + Cl$

$HOCl + h\nu \rightarrow OH + Cl$

$ClONO_2 + h\nu \rightarrow$ products

$CCl_4 + h\nu \rightarrow$ products

$CCl_3F + h\nu \rightarrow$ products

$CCl_2F_2 + h\nu \rightarrow$ products

$CH_3Cl + h\nu \rightarrow$ products

$CH_3CCl_3 + h\nu \rightarrow$ products

in the atmosphere, the solar irradiance is attenuated by absorption essentially by molecular oxygen and by ozone. Its value can also be altered by scattering effects and by the albedo of the Earth, especially for the wavelengths larger than 300 nm. Table 2 shows the most important photodissociation processes in the stratosphere.

3. DYNAMICAL AND THERMAL PROCESSES IN THE STRATOSPHERE

Long-lived traces such as CH_4, N_2O, CFCs, H_2O, H_2 in the whole atmosphere or such as water vapor in the lower part of the stratosphere are transported by air motion. Heat produced by sunlight absorption is also subject to atmospheric transport in different atmospheric regions. The description of the dynamical processes in the atmosphere is very complicated since one has to consider simultaneously mean motion, waves characterized by different scales, eddies, etc... and the mutual interactions between these various mechanisms. Since this paper is devoted mainly to chemical processes, only the general equations will be given hereafter.

3.1. Governing equations of atmospheric dynamics

The basic continuity equations of momentum and energy with proper boundary and initial conditions can in principle describe the detailed physical state of the atmosphere. These non linear partial differential equations, which apply in three dimensions, cannot be treated without severe approximations using the available computer facilities. The conservation of momentum and of energy may be written respectively as

$$\frac{d\vec{V}}{dt} + 2\,\vec{\Omega} \times \vec{V} + \frac{1}{\rho}\,\vec{\nabla}\,p = \vec{g} + \vec{F} \qquad (17)$$

$$\frac{dT}{dt} = \frac{1}{\rho C_p}\,\frac{dp}{dt} + \frac{Q}{C_p} \qquad (18)$$

where p is the pressure, ρ the density, T the absolute temperature, $\vec{V}$ air velocity, $\vec{\Omega}$ the Earth angular velocity, $\vec{F}$ the frictional force per unit mass, Q the net (diabatic) heating rate, $\vec{g}$ the apparent acceleration due to the Earth gravity and C_p the specific heat of air at constant pressure. It can be shown (see e.g. Brasseur, 1982) that these equations can be developed in three dimensional spherical coordinates as

$$\frac{\partial u}{\partial t} + \frac{u}{a \cos\varphi}\frac{\partial u}{\partial \lambda} + \frac{v}{a \cos\varphi}\frac{\partial}{\partial \varphi}(u \cos\varphi) + w\frac{\partial u}{\partial z}$$

$$- fv + \frac{1}{\rho\, a \cos\varphi}\frac{\partial p}{\partial \lambda} - F_\lambda = 0 \qquad (19.a)$$

$$\frac{\partial v}{\partial t} + \frac{u}{a \cos\varphi}\frac{\partial v}{\partial \lambda} + \frac{v}{a}\frac{\partial v}{\partial \varphi} + w\frac{\partial v}{\partial z} + \frac{tg\,\varphi}{a}u$$

$$+ fu + \frac{1}{\rho a}\frac{\partial p}{\partial \varphi} - F_\varphi = 0 \qquad (19.b)$$

$$\frac{\partial w}{\partial t} + \frac{u}{a \cos\varphi}\frac{\partial w}{\partial \lambda} + \frac{v}{a}\frac{\partial w}{\partial \varphi} + \frac{u^2}{a} + 2\,\Omega \cos\varphi\, u$$

$$+ g + \frac{1}{\rho}\frac{\partial p}{\partial z} - F_z = 0 \qquad (19.c)$$

$$\frac{\partial T}{\partial t} + \frac{u}{a \cos\varphi}\frac{\partial T}{\partial \lambda} + \frac{v}{a}\frac{\partial T}{\partial \varphi} + w\frac{\partial T}{\partial z}$$

$$- \frac{1}{\rho C_p}\left(\frac{\partial p}{\partial t} + \frac{u}{a \cos\varphi}\frac{\partial p}{\partial \lambda} + \frac{v}{a}\frac{\partial p}{\partial \varphi} + w\frac{\partial p}{\partial z}\right) = \frac{Q}{C_p} \qquad (20)$$

where a is the Earth radius, $f = 2\,\Omega \sin\varphi$ the Coriolis factor, λ, φ and z respectively the longitude, the latitude and the altitude, u, v and w respectively the zonal, meridional and vertical component of the wind velocity. These variables are not independent since the conservation of mass has to be satisfied through the following continuity equation

$$\frac{1}{a \cos \varphi} \frac{\partial u}{\partial \lambda} + \frac{1}{a \cos \varphi} \frac{\partial}{\partial \varphi} (v \cos \varphi) + \frac{\partial w}{\partial z} - \frac{w}{H} = 0 \qquad (21)$$

where $H \equiv kT/mg$ is the atmospheric scale height.

3.2. Thermal processes in the stratosphere

The heating rate in the stratosphere is due mainly to the absorption of ultraviolet radiation by ozone in the Hartley and Huggins bands. Its value depends critically on the concentration of O_3 and is given by (if expressed in K/day)

$$P = \frac{n(O_3)}{\rho C_p} \int_{\lambda} \sigma(O_3; \lambda) F(\lambda, z, \chi) \, d\lambda \qquad (22)$$

where F is the solar energy flux at wavelength λ, at altitude z and for a solar zenith angle χ.

The cooling of the atmosphere below 80 km is due mainly to the infrared emission of carbon dioxide in the 15 μm band. The contribution of the 9.6 μm band emission of ozone accounts for never more than 30-35 percent. In the stratosphere where local thermodynamic equilibrium applies, the cooling rate which is proportional to the Planck function is a direct function of the emitting gas temperature and reaches therefore a maximum near the stratopause. Fig. 6 shows the heating rate due to the different processes occuring in the stratosphere.

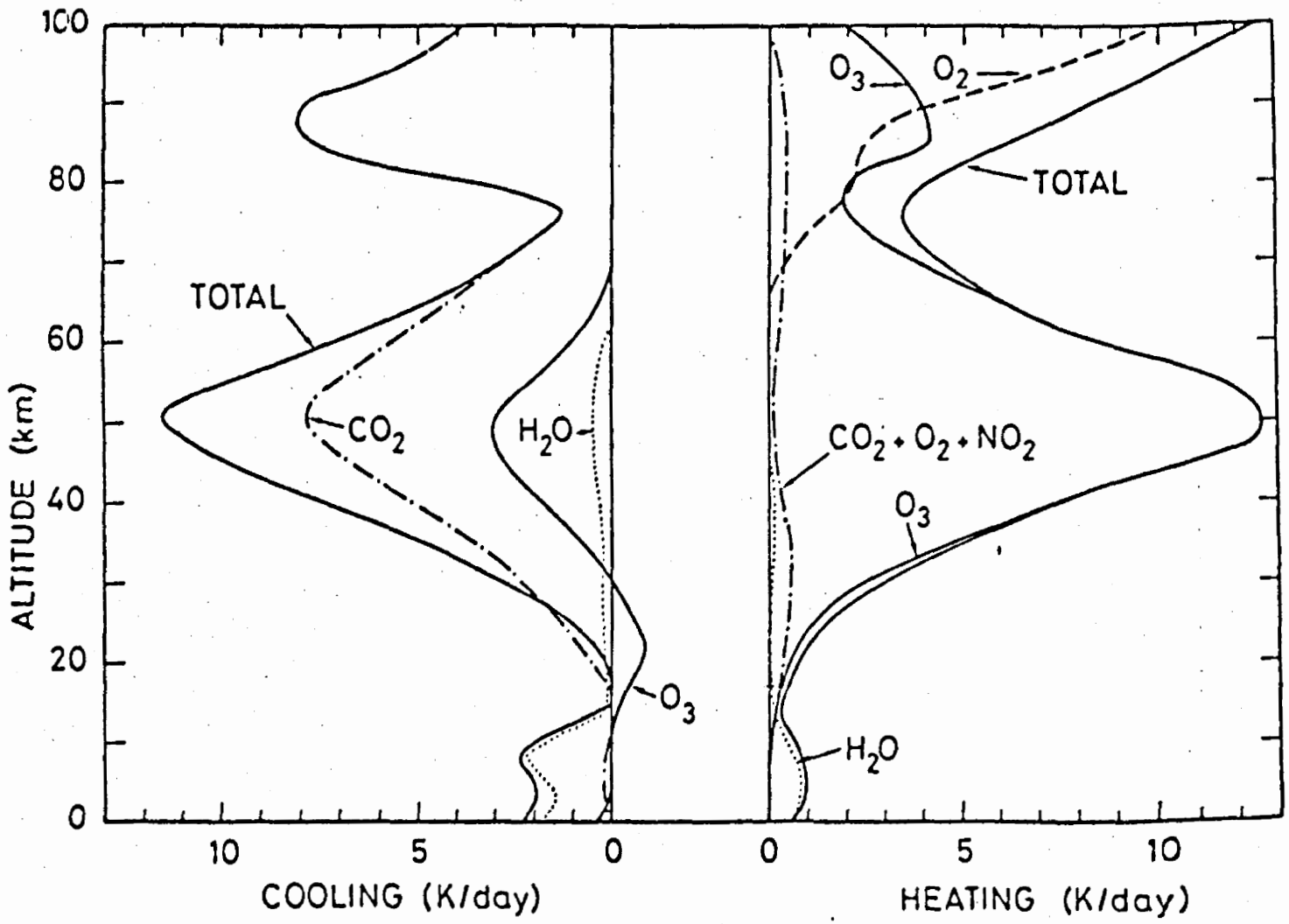

Fig. 6.- Different contributions of the heating and cooling rates in the atmosphere between 0 and 100 km.

4. MODELLING OF THE NATURAL OZONOSPHERE

The treatment of the governing equation requires a proper separation of the mean motions and of the waves. In some cases, the three-dimensional problem is reduced to a two-dimensional or even a one-dimensional representation. Even with these simplifications, valuable conclusions can be obtained.

One of the purposes of numerical models is to verify if the adopted chemical and photochemical scheme with its related rate constants takes into account the most important atmospheric processes. In order to achieve this goal, the concentration fields obtained theoretically are compared with the available observations. The discrepancies have to be attributed either to missing reactions, to errors in some reaction rates or to an inadequateness in the transport parametrization.

In the recent years, several numerical models have been developped with various degrees of sophistication. In the most comprehensive two or three dimensional models, detailled dynamical processes are considered as well as feedback mechanisms between chemical, radiative, thermal and dynamical aspects. One dimensional models which will be considered here give a simplified description of the chemical and photochemical processes in the atmosphere. They are useful to estimate, without prohibitive computer time, the sensitivity of the atmospheric composition to the numerous factors which are introduced as input data (rate constants, solar irradiance, absorption cross section, temperature, vertical exchange coefficients, boundary conditions, ...). In this case, the continuity equation (1) becomes

$$\frac{\partial n_i}{\partial t} + \frac{\partial \phi_i}{\partial z} = P_i - L_i \qquad (23)$$

where the vertical flux ϕ_i is usually parametrized by an effective diffusion equation, namely

$$\phi_i = - K\, n(M) \frac{\partial f_i}{\partial z} \qquad (24)$$

In this expression n(M) is the total atmospheric concentration, f_i is the volume mixing ratio of species i, z the altitud and K the so-called vertical exchange or eddy diffusion coefficient wh.ch can in principle be derived from dynamical considerations. Howev for practical reasons, this phenomenological parameter is usually derived by inverting the continuity/transport equation for long-lived trace species (such as N_2O or CH_4) whose vertical distribution is known with a certain degree of accuracy.

The 1-D models, despite the limitations of the K theory, have been extensively used in studying perturbations to the ozone layer. The purpose of this section is to describe the 1-D model used at the Aeronomy Institute and to present some of the most significant results. In order to validate the model, calculated and observed distributions will be compared.

4.1. Model description, simplifications and input

The model which extends up to 100 km altitude considers the chemical and photochemical reactions which are given in table 1 and 2. It can be run in two different versions :

1. a steady-state version in which $\partial/\partial t$ is put equal to zero.
2. a time-dependent version which does not consider daily or seasonal variations but which simulates the long term effect of a CFC injection.

Most results have been obtained with the first version which consumes little computer time. The main characteristics of the model are the following :

1. Physical domain of definition : the model extends from 0 to 100 km altitude in 1 km vertical steps..

2. Boundary conditions : the concentration or the flux of the long-lived species is held fixed at the lower and upper boundaries (see table 3). For perturbation calculations the flux of anthropogenic compounds produced at ground level is specified. For short-lived species, photochemical conditions are adopted and no boundary condition is required.

3. Transport parameters : The exchange coefficients (K) given by fig. 7 are adopted.

4. Chemical kinetics system : O_3, $O(^3P)$, $O(^1D)$, N_2O, N, NO, NO_2, N_2O_5, HNO_3, HO_2NO_2, H, OH, HO_2, H_2O_2, CH_4, CO, CH_3Cl, CCl_4, CF_2Cl_2, $CFCl_3$, Cl, ClO, HCl, HOCl, $ClONO_2$ are treated fully interactively while O_2, N_2, H_2O, H_2 and CH_3O_2 concentrations are specified.

5. Photodissociation coefficients : The photodissociation rates are computed for the following conditions : 24 hours average at 30 degrees latitude and at the equinox. Solar fluxes are from Brasseur and Simon (1981).

6. Diurnal variations : The diurnal variation of the concentration is not computed explicitly since the purpose of the model is to derive steady state values representing a 24 hours average. For some reservoir species such as N_2O_5 the average concentration is far from the concentration obtained with an average solar illumination. This constituent is quickly produced during the beginning of the night but its destruction during the day is very slow and its concentration never reaches a daytime equilibrium value. For such temporary reservoir, it is assumed in the model that the nighttime production is on the average balanced by the daytime destruction. When two constituents (say X and Y) with larger diurnal variations

TABLE 3 : Boundary conditions.

Constituent	Lower boundary (0 km)	Upper boundary (100 km)
N_2O	$f = 3.3 \times 10^{-7}$	$\phi = 0$
CH_3Cl	$f = 8.0 \times 10^{-10}$	$\phi = 0$
CH_4	$f = 1.5 \times 10^{-6}$	$\phi = 0$
CO	$f = 1.0 \times 10^{-7}$	$\phi = 0$
Cl_x	$f = 1.0 \times 10^{-9}$	$\phi = 0$
H	photochemical equilibrium	$f = 4.3 \times 10^{-6}$
NO_y	$f = 3.0 \times 10^{-9}$	$f = 5.4 \times 10^{-6}$
O_x $(O + O_3)$	$f = 3.0 \times 10^{-8}$	$f = 5.3 \times 10^{-2}$

(f = volume mixing ratio; ϕ = vertical flux).

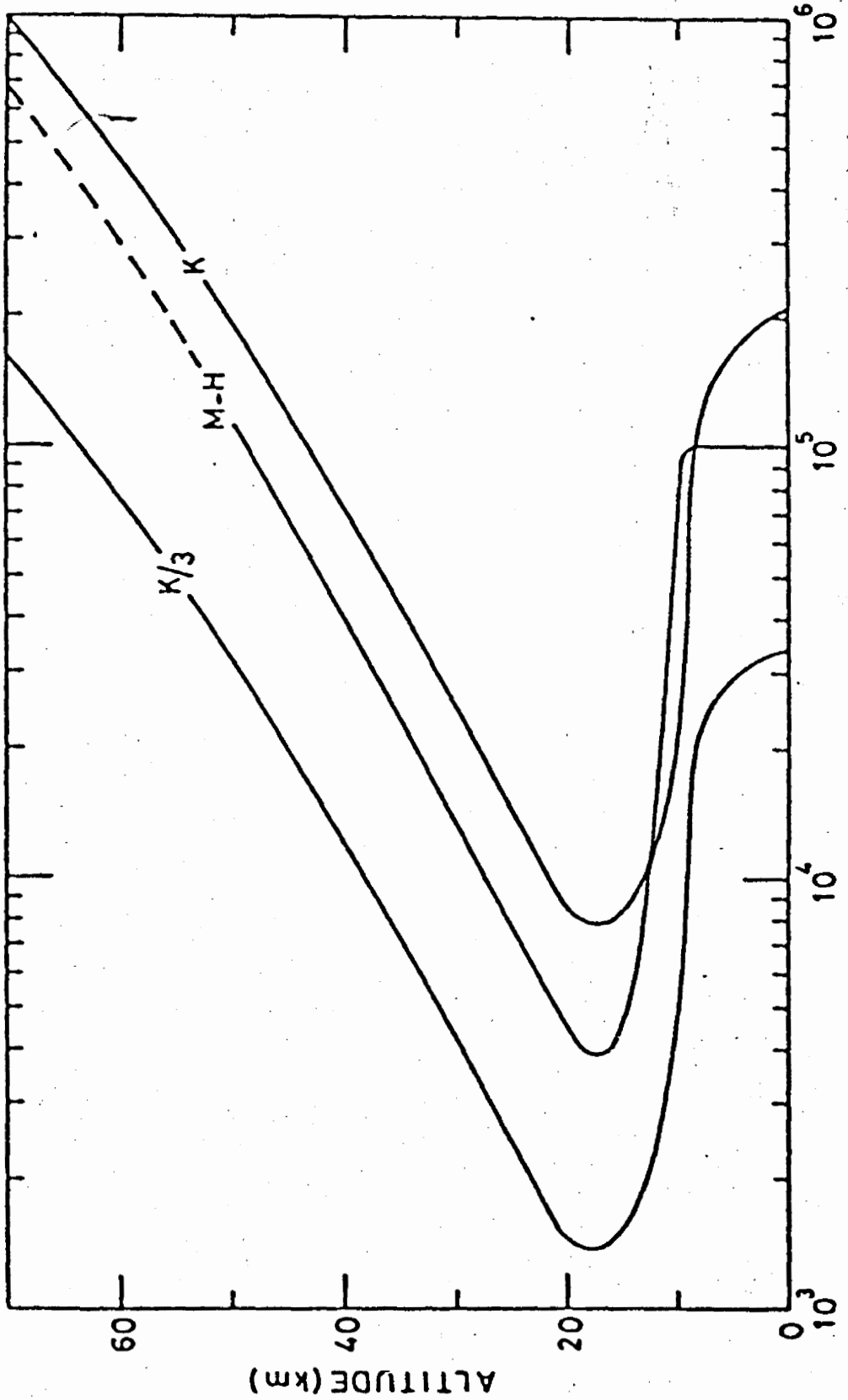

Fig. 7.- Adopted profiles of the eddy diffusion coefficient. The curve labelled K is used for most calculations.

are reacting together, the average of the product X.Y is different from the product of the mean values, namely $\bar{X}.\bar{Y}$. In this case, it is assumed in the model that

$$X.Y = \alpha \bar{X}.\bar{Y}$$

where α can only be determined from a detailed diurnal model. In the present work, the value of α for the different reactions (e.g. $NO_2 + O$ or $ClO + O$) has been imposed in accordance with the day/night variations obtained in current diurnal models. With such a parametrization, large time steps or steady state calculations can be used, taking into account the effect of the diurnal variation.

7. Other physical data : temperature are taken from the IAS reference model.

8. Numerical method : in order to avoid stiffness problems when solving the set of differential equations, the short-lived species are grouped into families (e.g. odd oxygen, odd nitrogen, odd chlorine, ...). Hence the fast rates due to the strong coupling of the individual constituents belonging to these families are eliminated. The different equations are then solved in sequence using a simple implicit discretisation technique. An iteration has to be performed in order to deal with the non linear terms. Species within the families are assumed to be in mutual photochemical equilibrium.

4.2. Model results

The interpretation of results provided by the 1-D model is not straightforward since the calculated concentrations are necessarily global averages over all latitudes and longitudes. Observations are obtained at specific locations and time and the comparison with calculated profiles is therefore not trivial. Furthermore a satisfactory

validation would require observational data of many chemical species obtained simultaneously. Since these conditions can not be achieved, the analysis of the calculated distributions can only be partial and no final conclusions can yet be drawn.

Fig. 8 shows for example the vertical distribution of the ozone concentration. This profile is in rather good agreement with some observations : the maximum value is located at 23 km with a corresponding value of 4.5×10^{12} cm^{-3}. The calculated ozone column is of the order of 345 Dobson units which corresponds to the value observed at 45° degrees latitude by Krueger an Minzner (1976). This number is very sensitive to the chemistry used, even if the shape of the profile remains almost the same when current changes are introduced in the values of the rate constants. For example, the ozone column is a function of the tropospheric production of O_3 and consequently to the calculated concentrations of NO, HO_2, and CH_3O_2 which are poorly known below 15 km. For these reasons, a detailed tropospheric 2-D model is under elaboration at the Aeronomy Institute. Furthermore, the shape of the ozone profile around and below the tropopause is determined by the value of the eddy diffusion profile and its gradient.

Fig. 9 represents the distribution of O_3 between 0 and 32 km for different representations of the transport across the tropopause. The corresponding (downward) fluxes at 12 km are the following : $- 6.3 \times 10^{10}$ cm^{-2} s^{-1} for the standard case labelled K, $- 1.6 \times 10^{10}$ cm^{-2} s^{-1} when K is divided uniformly by 3 and $- 3.0 \times 10^{10}$ cm^{-2} s^{-1} for the Massie and Hunten profile of K.

The intensity of the ozone destruction by chlorine compounds is directly related to the emission, transport and photodestruction of the chlorofluorocarbons. The most important of them, namely CCl_4, CF_2Cl_2, $CFCl_3$, CH_3CCl_3 are considered by the model as well as the natural CH_3Cl. For the conditions corresponding to the present time, a fixed mixing ratio based on the observations is prescribed as lower boundary condition (see table 4).

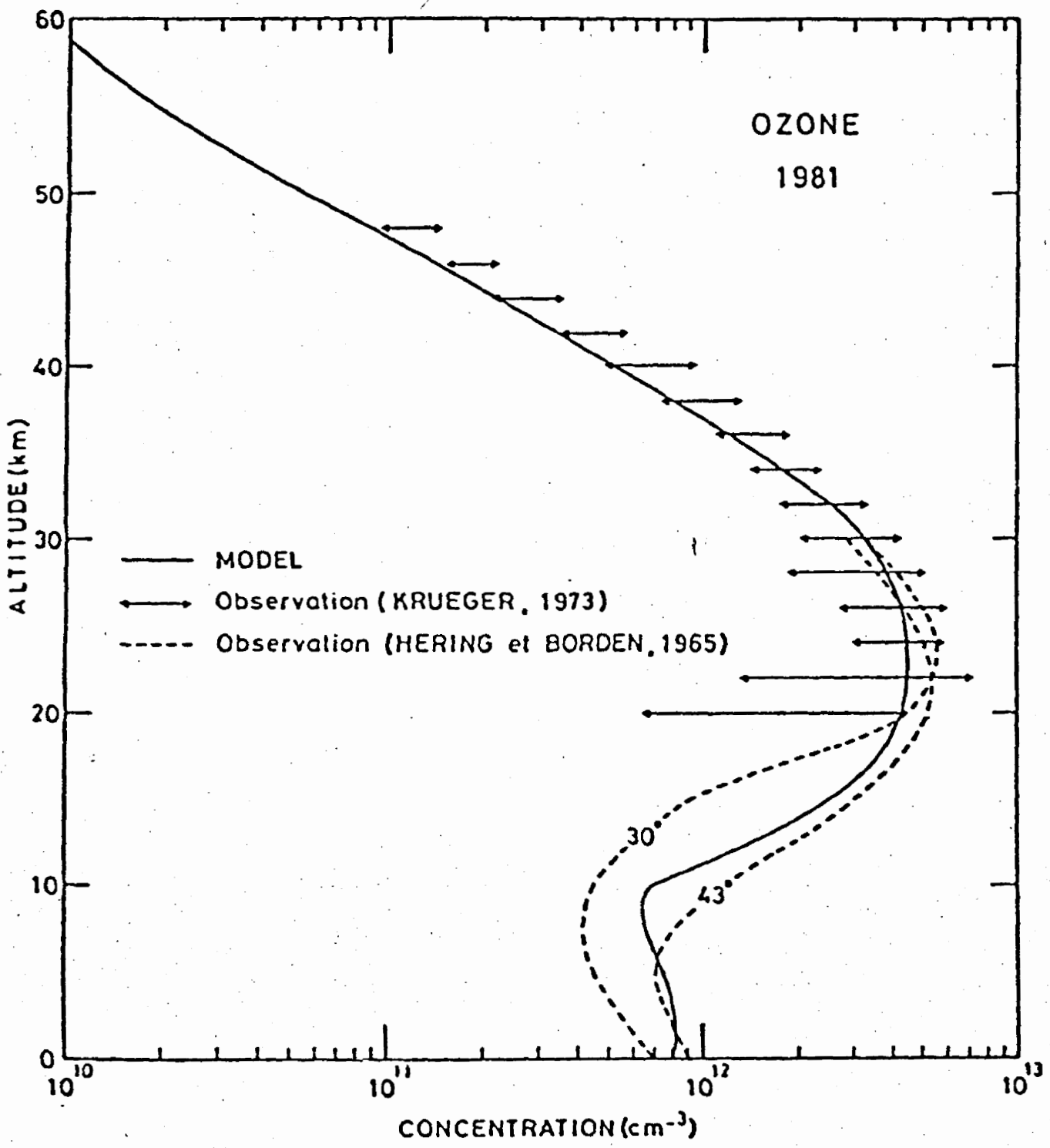

Fig. 8.- Calculated vertical distribution of ozone when the chemistry of table 2.1 is adopted. Comparison with observations.

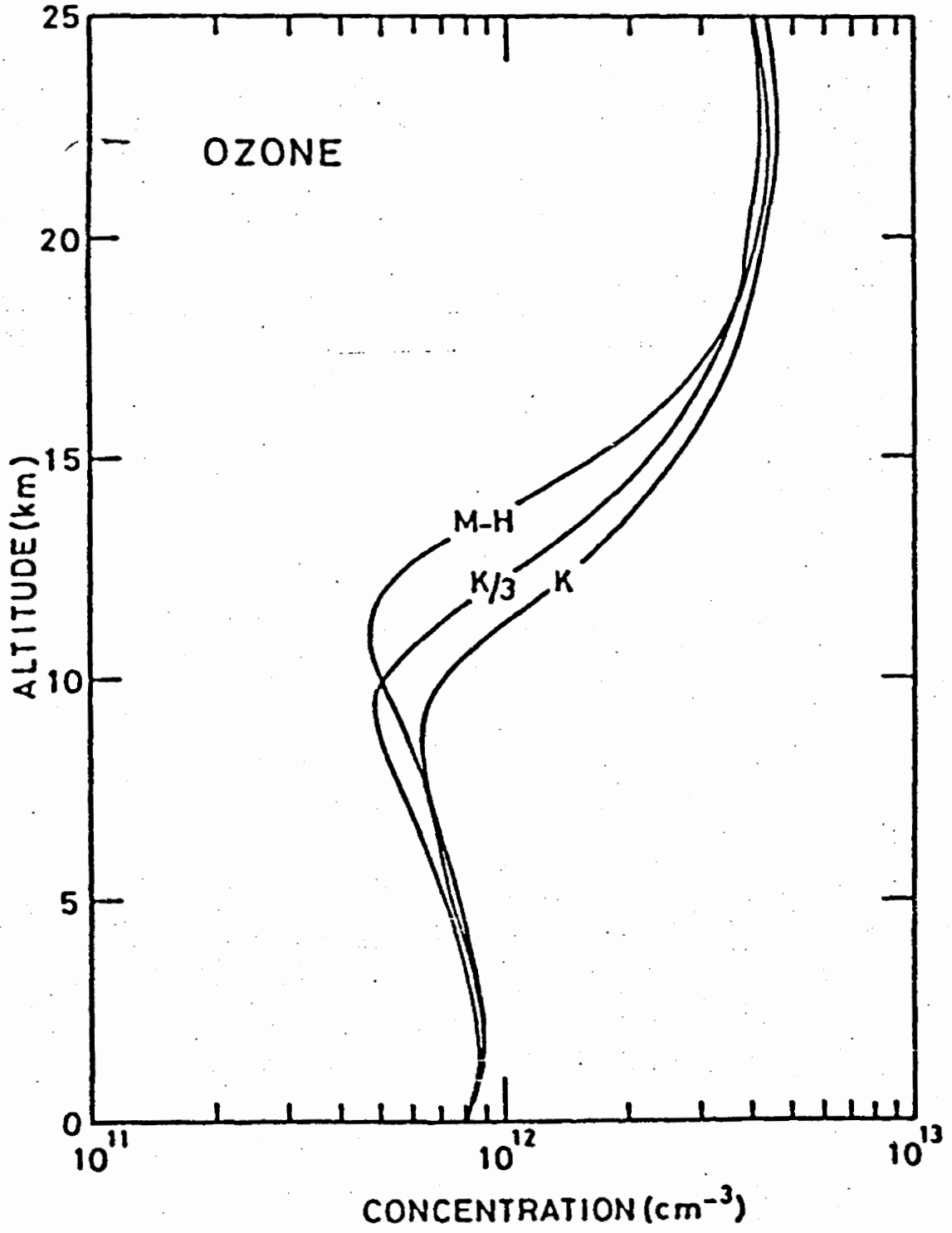

Fig. 9.- Effect of the K value on the ozone distribution in the vicinity of the tropopause.

TABLE 4 : Boundary conditions of the CFCs at the ground for the "present day" atmosphere.

CH_3Cl	8×10^{-10}
CCl_4	1.5×10^{-10}
$CFCl_3$	1.6×10^{-10}
CF_2Cl_2	2.8×10^{-10}
CH_3CCl_3	6×10^{-11}

The mixing ratio of the total chlorine is thus equal to 2.6 ppbv. Fig. 10 compares the distribution of the various chlorocarbons of stratospheric interest. Fig. 11, 12 and 13 compare the calculated profiles with some available observations taken in southern France. It can be seen immediately that the model predicts concentration values which are considerably higher than the observations (a factor of 3 or so in the upper levels). The reasons for these discrepancies which appear in all current models are yet unclear but several hypothesis can be done. For example, the intensity of the adopted vertical exchange coefficient can be overestimated. In fact, the results obtained when this coefficient is uniformly divided by 3 are in much better agreement with the observations. However, other problems will appear with other constituents, such as carbon monoxide around the tropopause and in the upper stratosphere (fig. 14).

Another reason for the discrepancy between model and observations could be an overestimation in the solar absorption which takes place in the Schumann-Runge bands of molecular oxygen. This spectral range plays an important role in the photodestruction of halocarbons, especially in the middle and upper part of the stratosphere. If this reason was proved to be right, it could probably also explain the discrepancies occuring in the case of nitric acid. However the determination of the Schumann-Runge bands absorption has been done carefully by Nicolet and Peetermans (1980) and Frederick and Hudson (1979). Both analysis done separately lead to more or less the same absorption values. Further work is needed because of the potential errors both in the fine structure of the Schumann-Runge bands and in the model representation of the absorption. Finally, it should be noted that most calculations related to the present day atmosphere do not consider the fact that the presently observed distribution of CFCs has not reached any steady state and these profiles are instantaneous pictures of an evoluting process related to the source strength (and its evolution) at ground level.

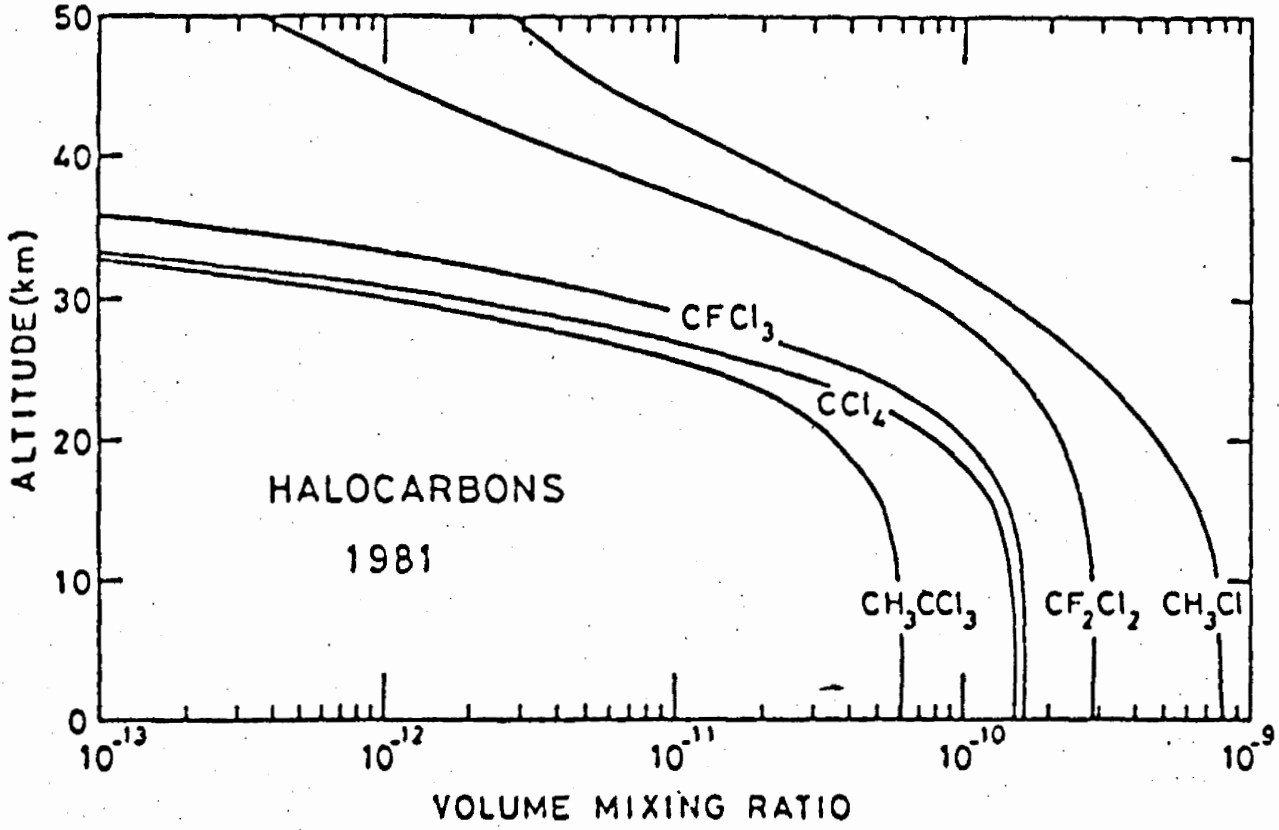

Fig. 10.- Mixing ratio of several halocarbons as a function of the altitude. Present day conditions.

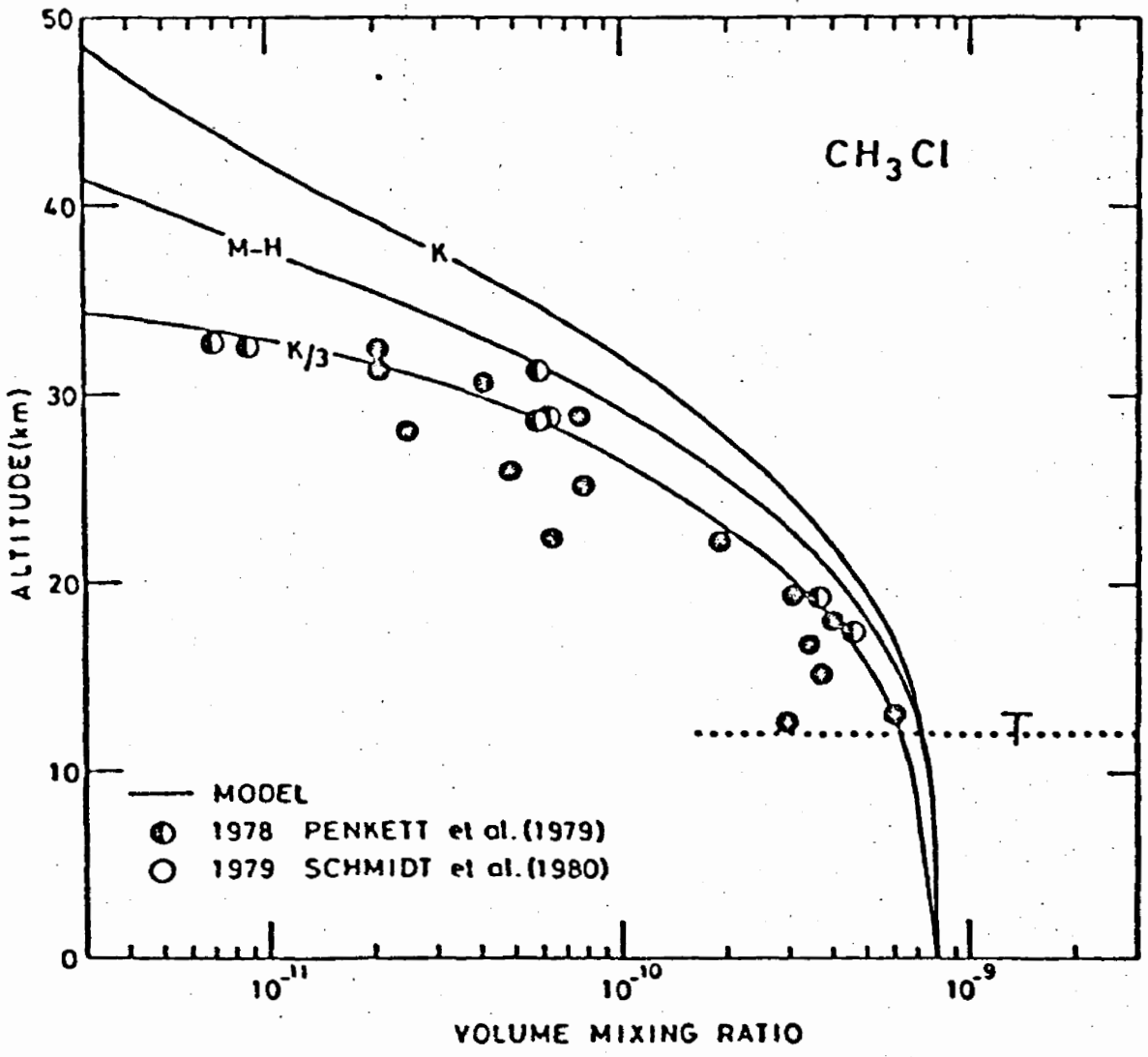

Fig. 11.- Comparison between observed and calculated mixing ratio of CH_3Cl. Effect of different exchange coefficients.

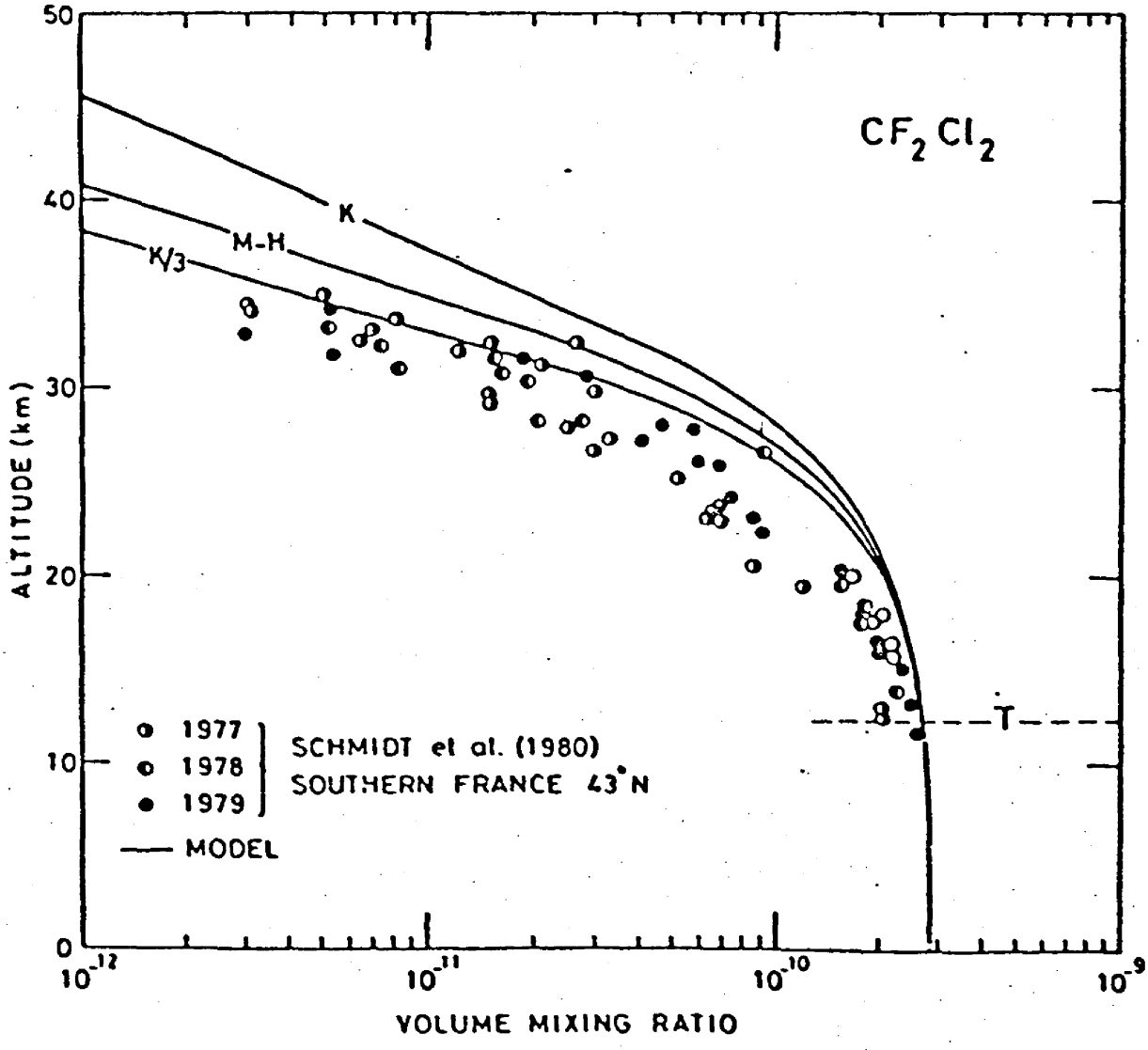

Fig. 12.- Same as fig. 3.4 but for CF_2Cl_2.

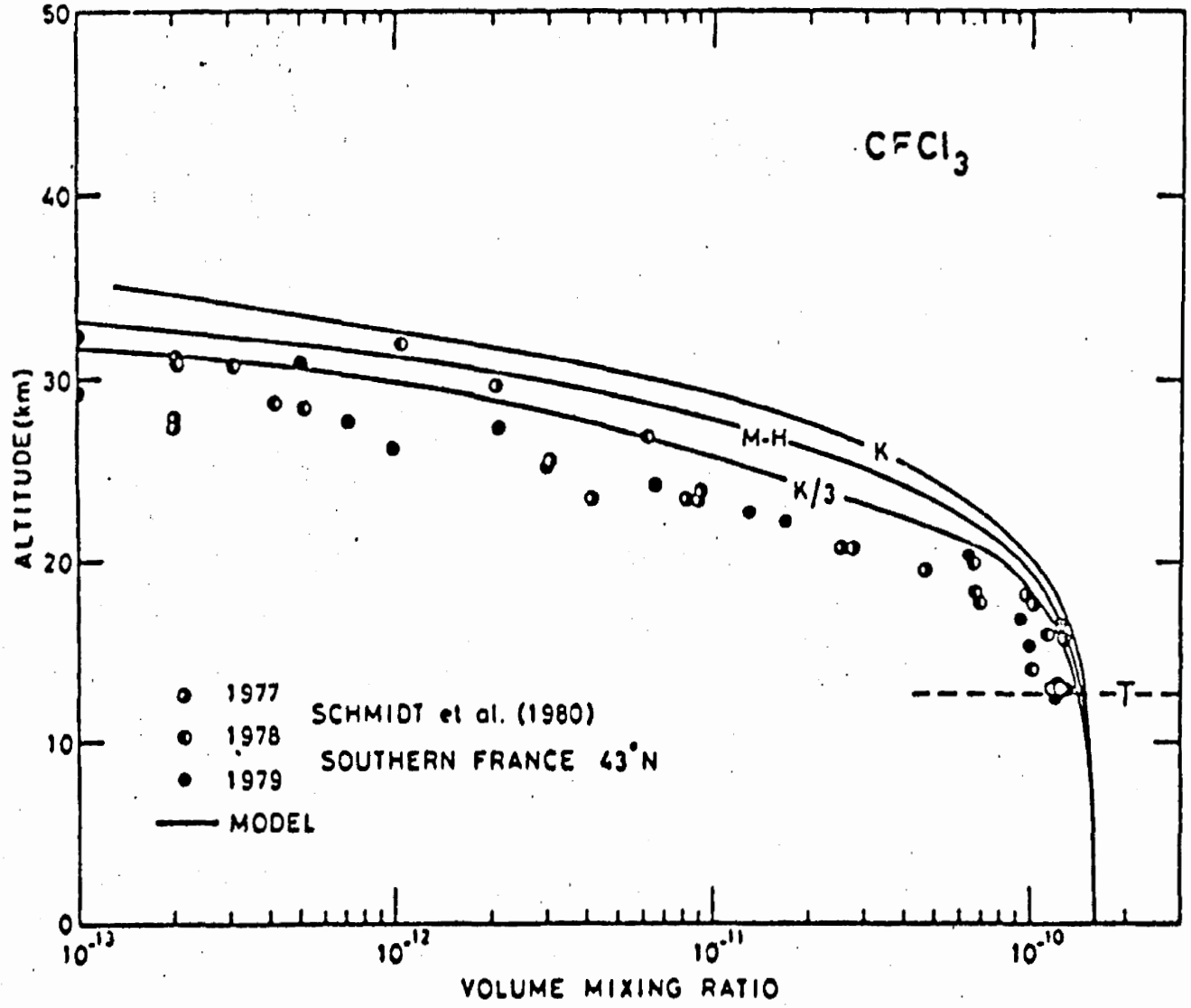

Fig. 13.- Same as fig. 3.4 but for $CFCl_3$.

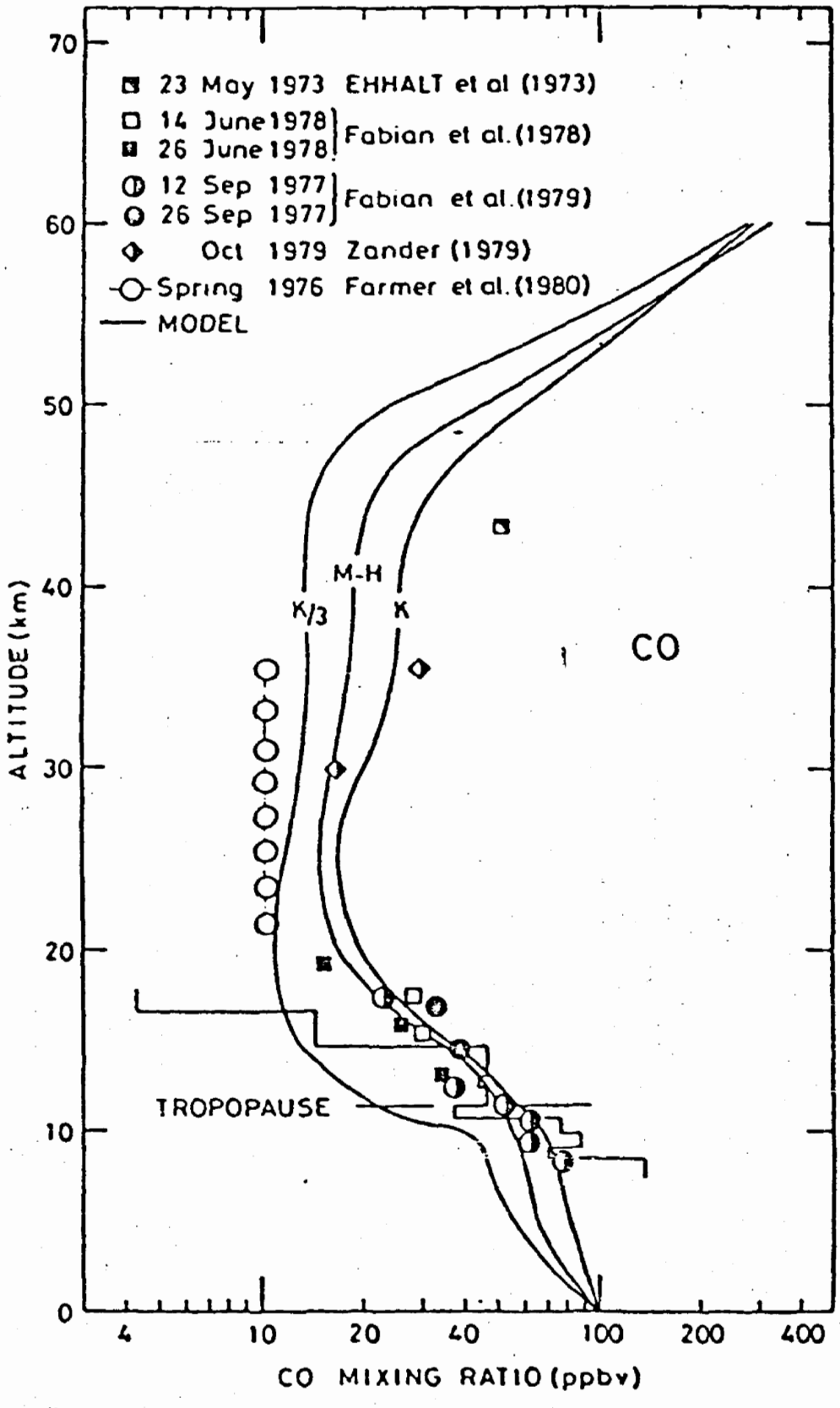

Fig. 14.- Vertical distribution of the CO mixing ratio calculated for three exchange coefficients. Comparison with the observation.

The atmospheric concentrations of ClO is of great importance since the loss rate of ozone is directly related to its value. The comparison between observation and theory is not straightforward since the measurements show a large scatter which is not yet explained. Fig. 15 shows that the general shape of the distribution is rather well represented by the model below 30-35 km but that it is not the case anymore in the upper stratosphere (above 35-40 km) where the calculated mixing ratio gradient becomes negative, contrary to most observations. In fact, the calculated profile falls toward the high end of the observation between 25 and 35 km (if the two abnormal measured profiles are excluded) and toward the low value at 40 km. The discrepancy of the ClO distribution is one of the main problems whic will have to be solved in order to give some credibility to the predictions in relation to the CFCs perturbations. At the present time, the models seem to underestimate the amount of chlore in the upper stratosphere. Fig. 15 also shows the sensitivity of ClO to the K profile. The enhancement of the ClO mixing ratio when K is divided by 3 is due to the reduction of the methane concentration and therefore to the slow down of the conversion of Cl into HCl.

The comparison of theoretical and observed values has changed quite substantially in the recent months. The recent appearance of new values of the destruction rate of OH by HNO_3, HO_2NO_2 and H_2O_2, leading to a smaller amount of OH and consequently to a smaller ClO concentration, which is closer to the average observation below 30 km. However, the results have become really unsatisfactory in the upper stratosphere.

The calculated distribution of CH_4 is shown in fig. 16 and is compared to observations performed at 32°N (Palestine, Texas) and 44°N (Aire sur l'Adour, France). Due to the rather large scatter in the observations, it is not clear what eddy diffusion coefficient is the most convenient. For instance, the profile of Massie and Hunten represents well the observation by Ackerman et al (1978). However, even when a high value of K is adopted, the calculated concentrations are

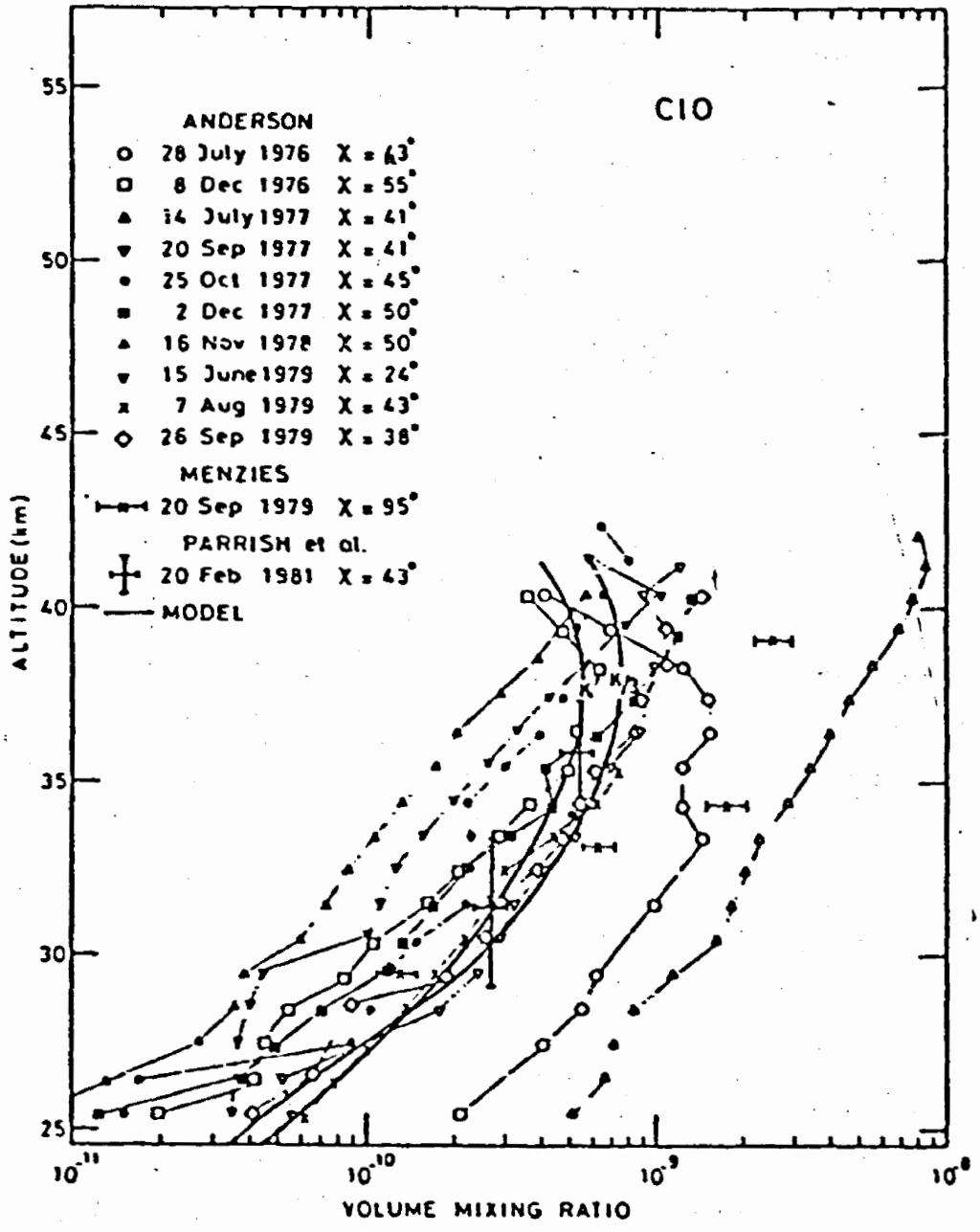

Fig. 15.- Comparison of observed and calculated mixing ratio of ClO.

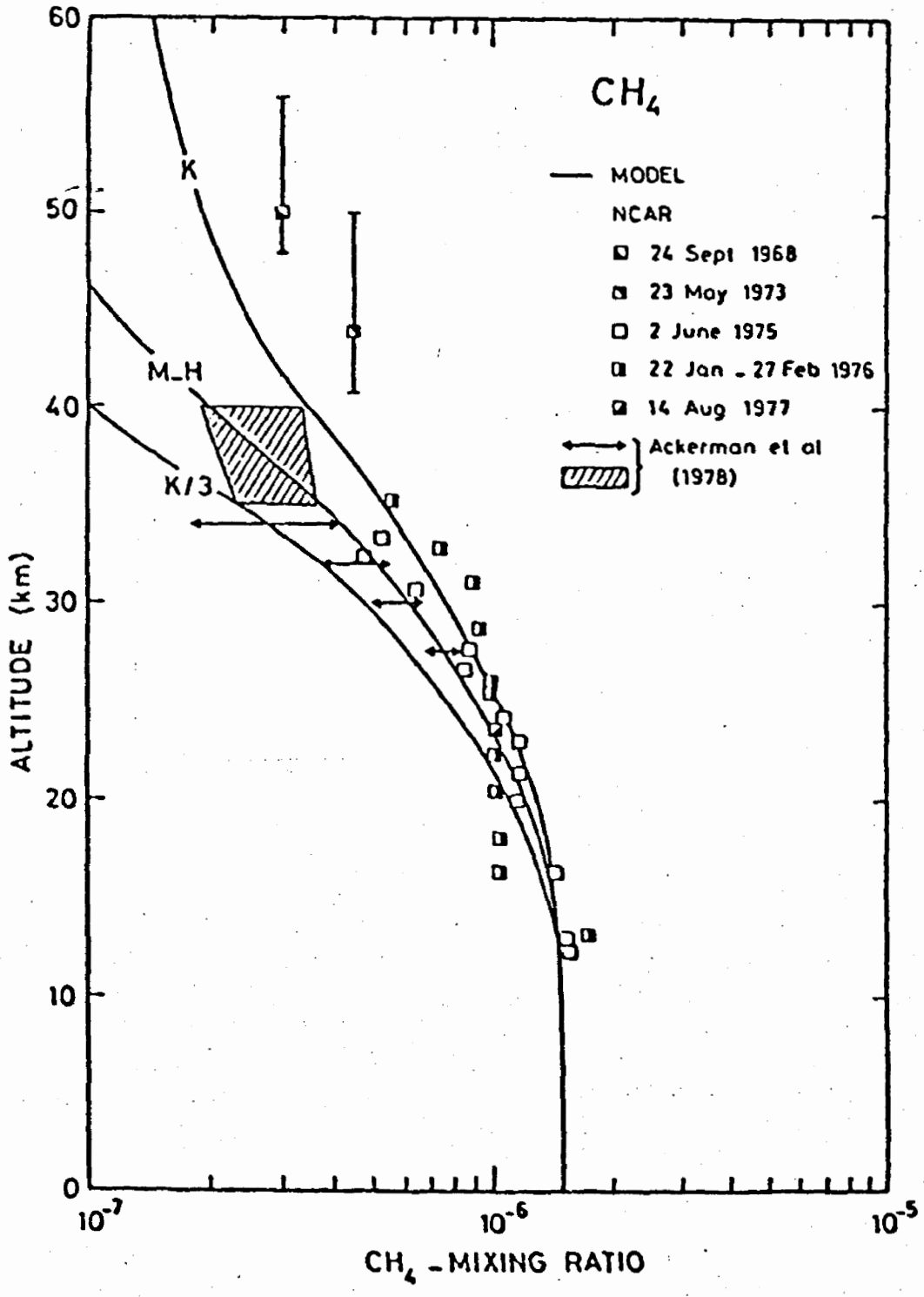

Fig. 16.- Same as fig. 3.4 but for CH_4.

much lower than the values observed by rockets around the stratopause. This problem also remains open.

When nitrous oxide is considered, in particular the mixing ratio measured at mid-latitude (see fig. 17), it is also difficult to give a preference to one of the exchange coefficient profiles. In fact, for all these long-lived trace species, continuous observations are needed, at different latitudes and in relation with the general circulation.

The distribution of most stratospheric compounds is directly related to the behavior of fast reacting odd hydrogen compounds, namely H, OH, HO_2, H_2O_2. In order to compute an exact value of the concentration of these species, the balance between the production and the destruction has to be established. The production rate is proportional to the concentration of $O(^1D)$ which is produced by ozone photodissociation and to the concentration of H_2O, CH_4 and H_2. The distribution of water vapor is highly dependent on the location and the dynamical conditions of the atmosphere and it is quite difficult to prescribe an average distribution. The absolute value of the H_2O mixing ratio at the stratopause is particularly poorly known due to the lack of observations. The loss rate of odd hydrogen in the middle and upper stratosphere is due essentially to the recombination of OH with HO_2. However, in the lower stratosphere and in the troposphere, one has to consider the reaction of OH with HNO_3, HO_2NO_2 and H_2O_2.

The rate constants of these reactions are not well known even if the knowledge of the quantitative values referring to these rate constants have been improved very recently. Three cases have been considered for the computations :

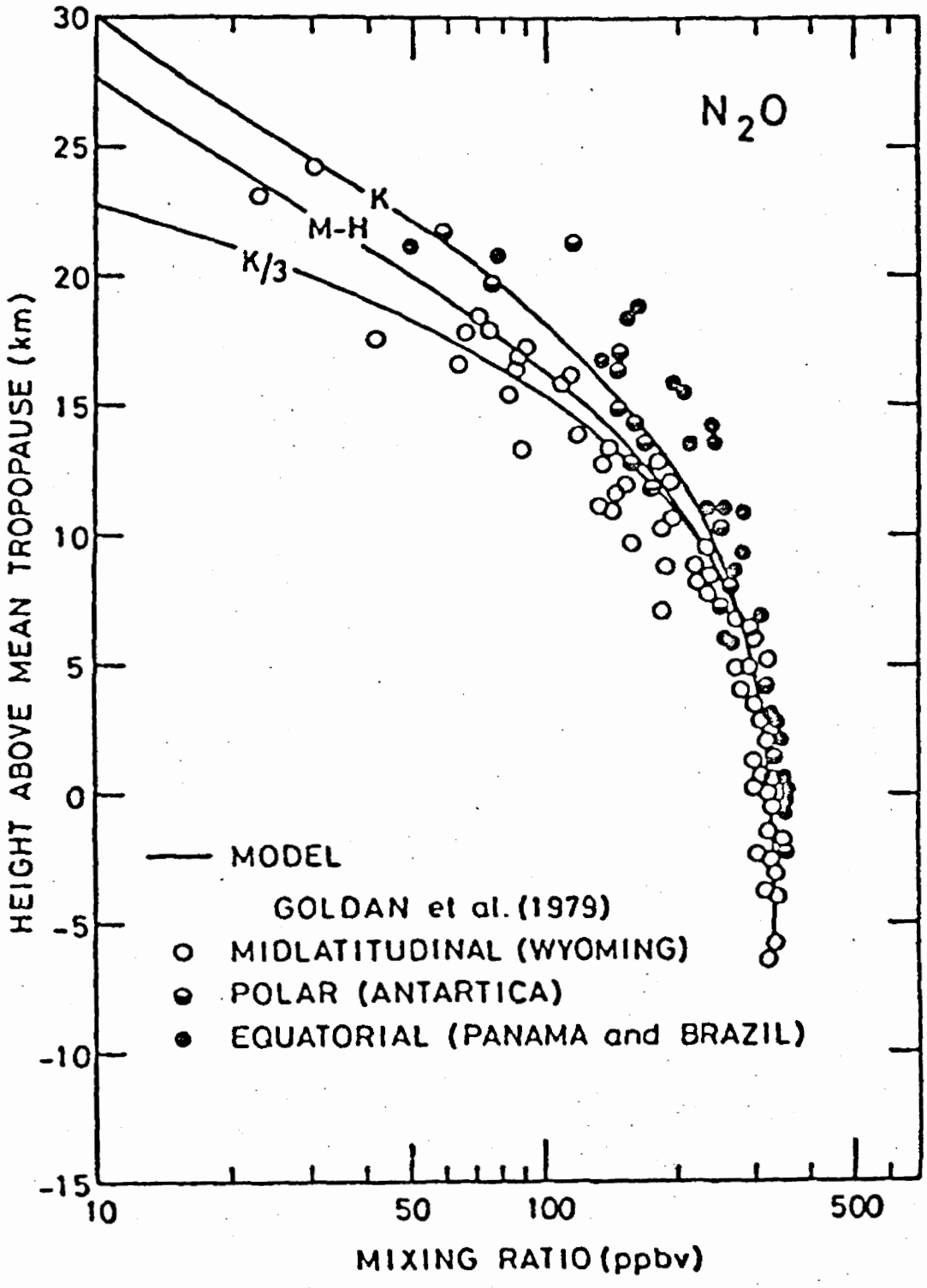

Fig. 17.- Same as fig. 3.4 but for N_2O.

Case 1

$OH + HO_2$	$a_{17} = 4 \times 10^{-11}$ cm^3 s^{-1}
$OH + HNO_3$	$b_{27} = 9 \times 10^{-14}$ cm^3 s^{-1}
$OH + HO_2NO_2$	$b_{30} = 5 \times 10^{-13}$ cm^3 s^{-1}

Case 2

$OH + HO_2$	$a_{17} = 1.5 \times 10^{-10}$ cm^3 s^{-1}
$OH + HNO_3$	$b_{27} = 1.5 \times 10^{-14}$ exp (649/T) cm^3 s^{-1}
$OH + HO_2NO_2$	$b_{30} = 4 \times 10^{-12}$ cm^3 s^{-1}

Case 3

$OH + HO_2$	$a_{17} = 8 \times 10^{-11}$ cm^3 s^{-1}
$OH + HNO_3$	$b_{27} = 1.5 \times 10^{-14}$ exp (649/T) cm^3 s^{-1}
$OH + HO_2NO_2$	$b_{30} = 4 \times 10^{-12}$ cm^3 s^{-1}

Case 3 refers to the recent recommendation of NASA which is presently widely accepted. Case 1 considers a slow destruction rate of HO_x and is thus representative of the 1979 chemistry. Finally case 2 uses a fast recombination of HO_x and leads thus to low values of the odd hydrogen concentrations. The sensitivity of the OH concentration to these changes is described in fig. 18.

Finally, fig. 19 to 21 represent the calculated mixing ratio of NO, NO_2 and HNO_3 as well as some observations. The agreement is rather good for NO even if a more careful model description is needed below 25 km and own in the troposphere. The calculation for NO_2 leads to acceptable values below 40 km but to relatively small values in the upper stratosphere. In this region most of the NO is converted into NO_2 during the night and a detailed diurnal study would be useful. Again the disagreement between the several observations makes the analysis rather complicated. Finally, one can see in fig. 21 that the agreement between

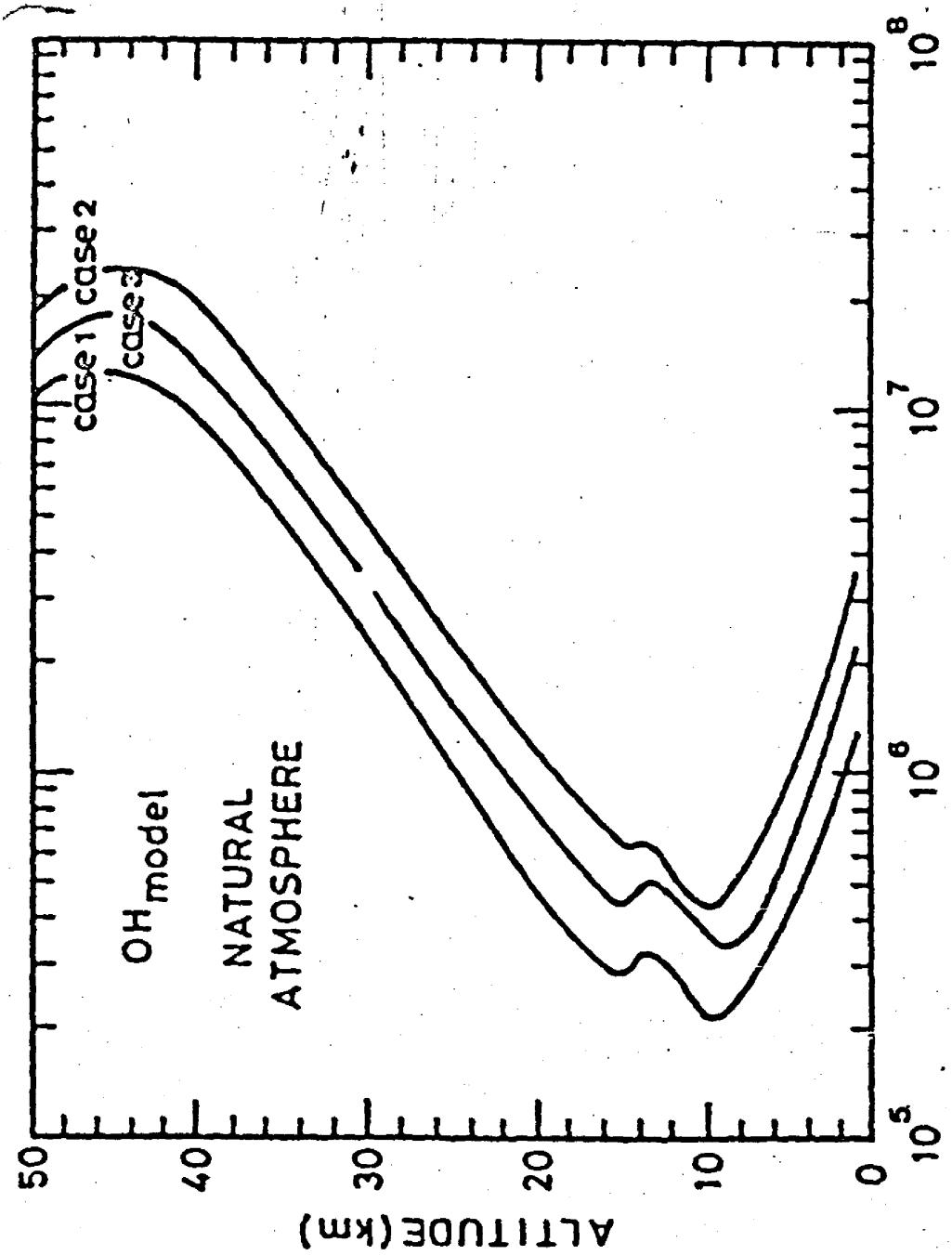

Fig. 18.- Vertical distribution of the OH concentration for three different chemical schemes.

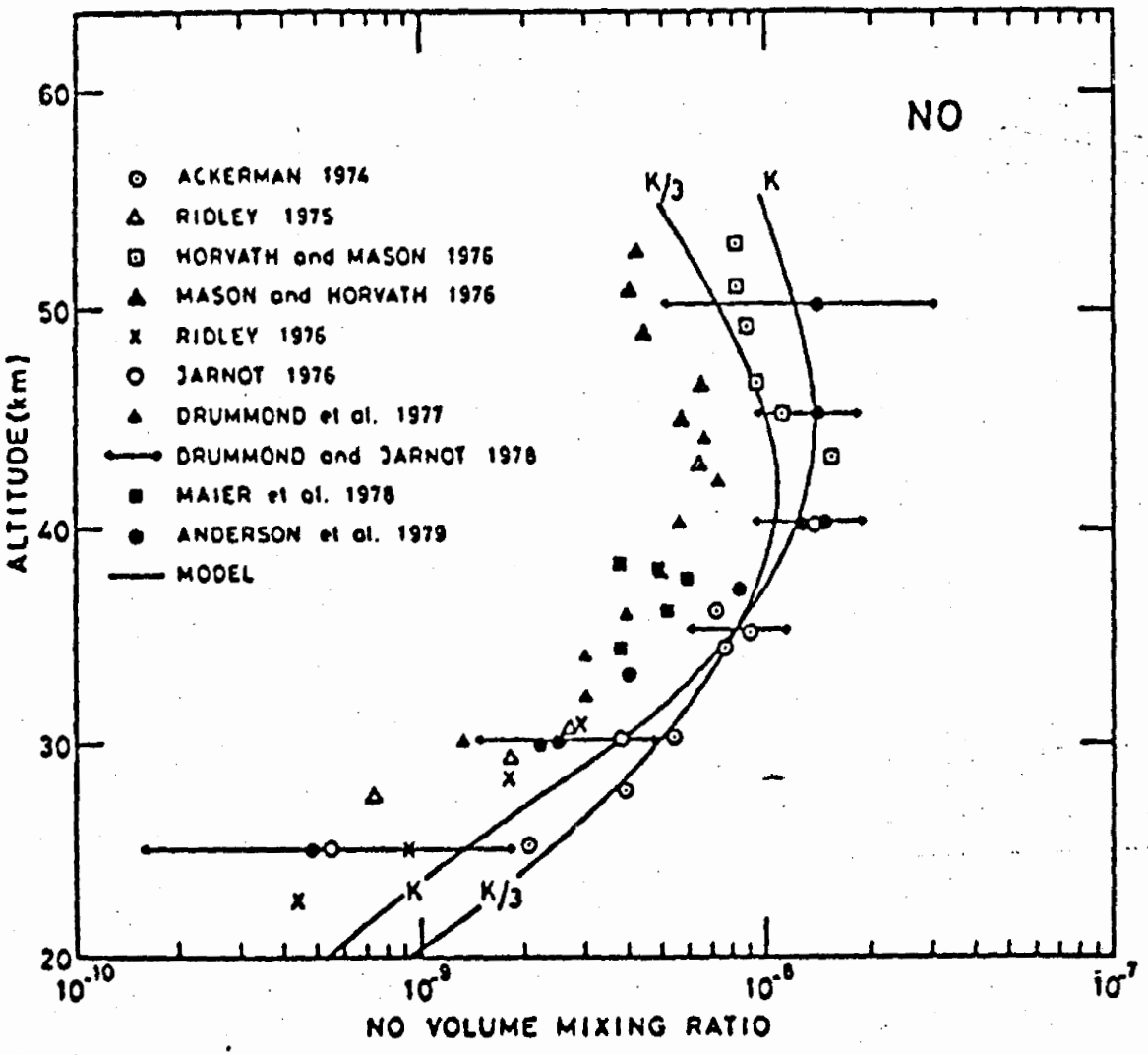

Fig. 19.- Comparison of observed and calculated NO mixing ratio as a function of altitude.

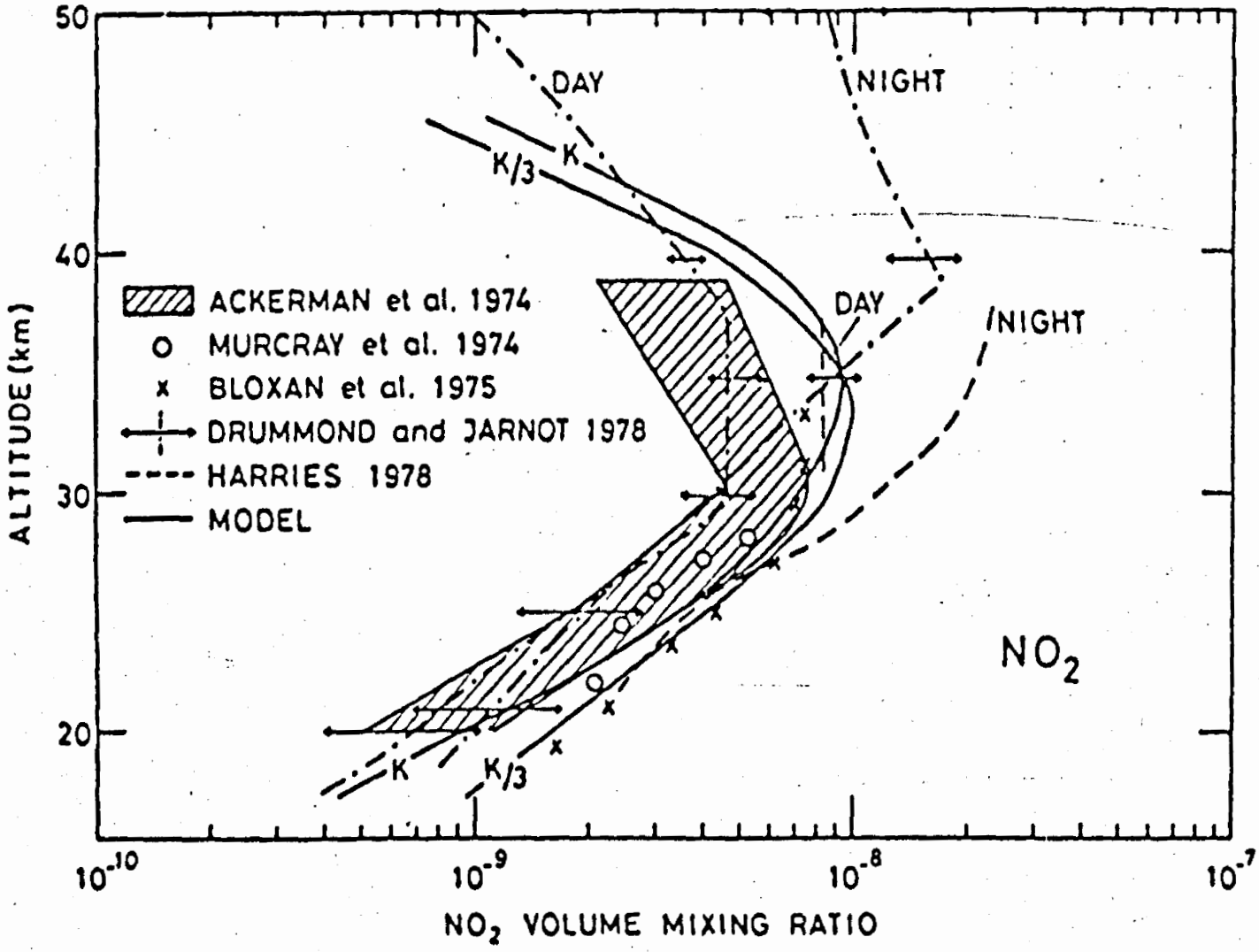

Fig. 20.- Same as fig. 3.11 but for NO_2.

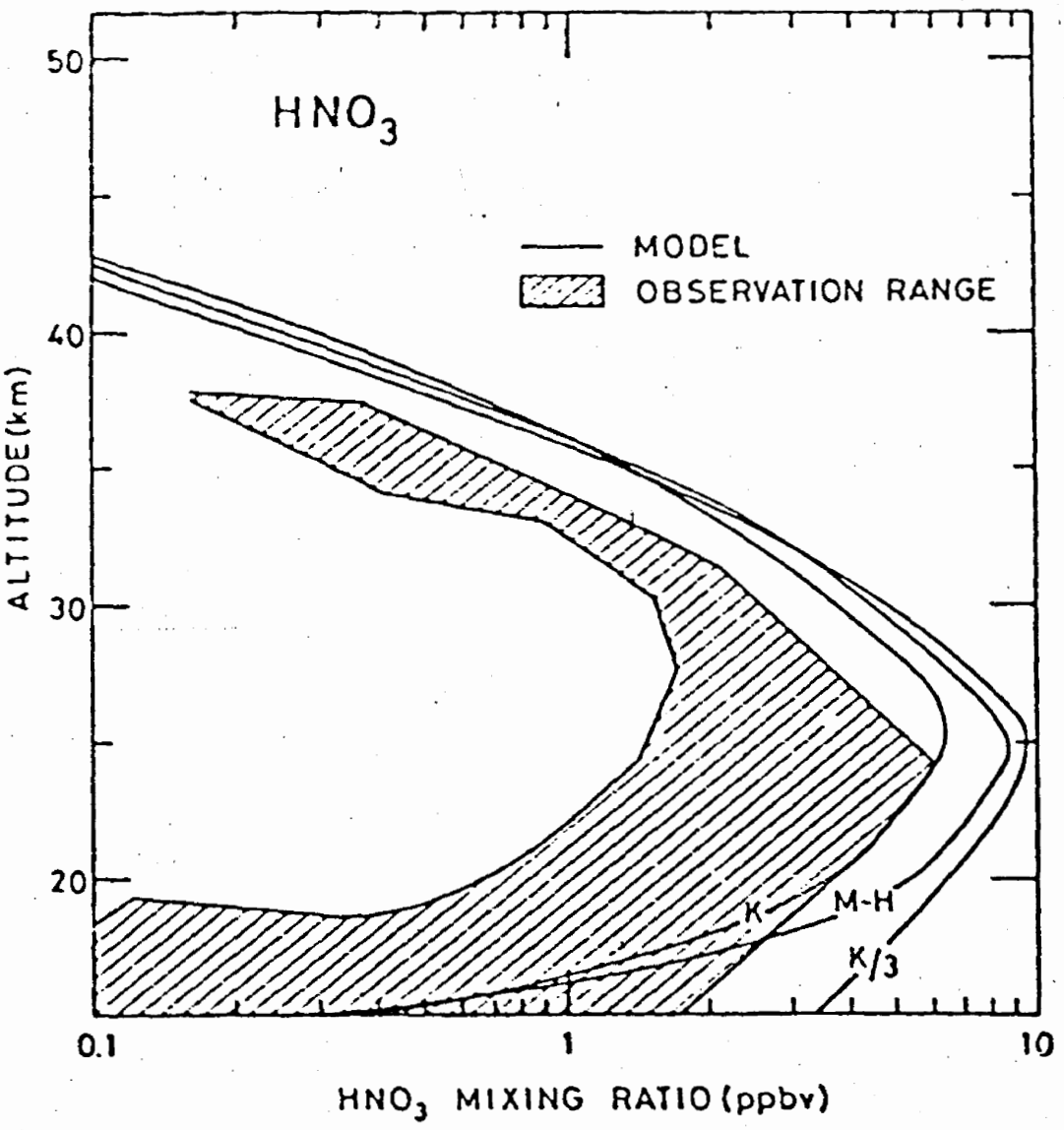

Fig. 21.- Same as fig. 3.11 but for HNO_3.

observed and calculated HNO_3 is poor above 25 km. There is a need for a stronger destruction mechanism or a weaker production process in the upper stratosphere. In the vicinity of the tropopause, the concentration of nitric acid depends very much on the intensity of the wash-out mechanisms and of the downward transport. The problem remains open. Below 30 km, the ratio between the HNO_3 and NO_2 concentration (fig. 22) is well represented and there has been a great improvement with the introduction of the recent values of the rate constants.

The main conclusion is that 1-D models give a general picture of the chemical processes occuring in the stratosphere and provide concentrations with an order of magnitude which is compatible with most observations. However, severe disagreements remain and these appear essentially in the upper stratosphere, i.e. in a chemically controlled region. Last year, the upper stratosphere was believed to be almost explained with the current chemistry while the description of the lower stratosphere was much poorer. With the updated reaction rates, the representation of the concentration values in the lower layers has been considerably improved but discrepancies appear above 35 km in the chemically active region. Further investigation is needed with a special emphasis on the variability near the stratopause and the interactions between the stratosphere and upper regions such as the mesosphere and the thermosphere. At the present time, the most important problems which have to be solved are the following :

1. The discrepancy of the CFCs in the middle and upper stratosphere
2. The probable theoretical underestimation of the chlorine amount in the present atmosphere. Observations of HCl and ClO seem to indicate a 3 ppbv mixing ratio of ClX at the stratopause. An underestimation of the chlorine release (natural or man-made) could explain this discrepancy.
3. The differences between the calculated and observed ClO profiles.
4. The large theoretical overestimation of nitric acid above 30 km and the discrepancy between observed and calculated NO_2 in the upper stratosphere.

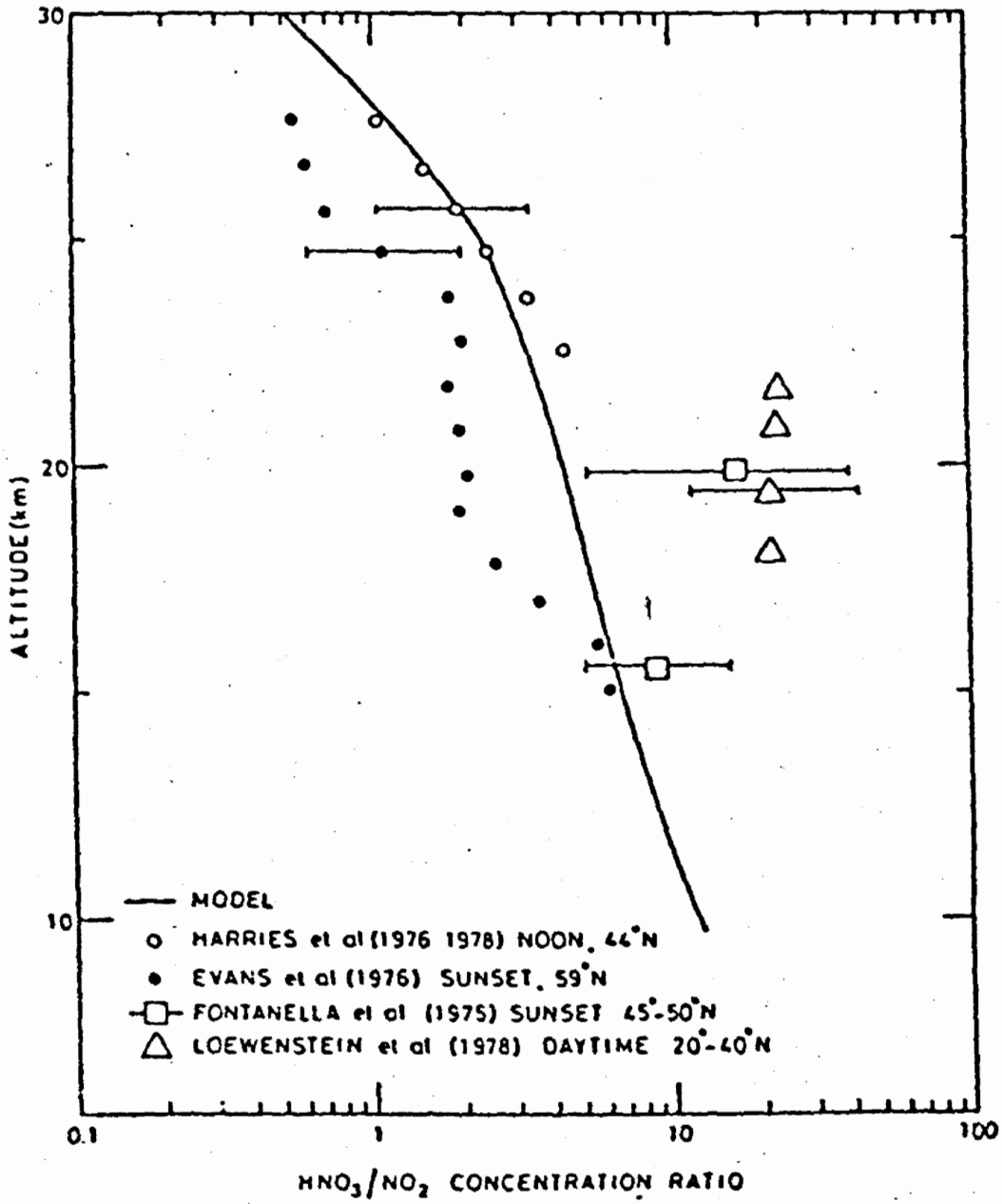

Fig. 22.- Ratio between the HNO_3 and NO_2 concentration. Comparison between observed and calculated values.

5. An exact determination of OH and HO_2 in the entire stratosphere (and mesosphere).
6. The water vapor behavior as a function of altitude, latitude and season.
7. The exact balance between production, destruction and transport of ozone in the lower stratosphere and in the troposphere.

4. EFFECT OF MAN-MADE PERTURBATIONS ON THE OZONE LAYER

Different chemical compounds which are produced by anthropogenic activities are released in the atmosphere and can be destroyed by several reactions to produce active radicals X which destroy ozone through the catalytic cycle :

$$X + O_3 \longrightarrow XO + O_2$$
$$XO + O(^3P) \longrightarrow X + O_2$$

$$\text{net} \quad O_3 + O(^3P) \longrightarrow 2O_2$$

For example, the release at ground level of chlorofluoromethanes, which have a large lifetime in the troposphere, leads to the formation of chlorine atoms (X = Cl) in the stratosphere. On the other hand, nitric oxide (X = NO) can be directly introduced by aircraft engines. In this case the source is located at the flight altitude in the upper troposphere or in the lower stratosphere. Most subsonic aircrafts enter the stratosphere only at relatively high latitude. Supersonic aircrafts such as Concorde fly around 15-17 km. A few military airplanes can fly higher in the stratosphere. Finally, one has to consider the wide use of fertilizers which increase the production of nitrous oxide at ground level. N_2O reacts with $O(^1D)$ atoms to produce NO molecules.

4.1. Potential changes in the ozone amount due to chlorofluorocarbon emissions

The sensitivity of the ozone layer to the chlorofluorocarbons is a critical function of the chemical scheme which is adopted and depends in particular on the rate constants describing the most important aeronomical reactions. The numbers for the ozone depletion, obtained by the models in the recent years, have changed quite a lot while new data became available from laboratory work. For example, adopting the 1976 release rate of CFCs as a permanent emission rate, it was felt two years ago that the steady state ozone depletion was of the order of 16 percent. At the present time, a 4 to 7 percent ozone reduction is currently accepted for the same emission strength.

In the present calculation, it is assumed that CH_3Cl, which is presently the most abundant chlorine species in the troposphere, is of natural origin and a constant mixing ratio of 0.8 ppbv is prescribed as lower boundary condition at ground level. The contribution of anthropogenic odd chlorine is provided by the presence of $CFCl_3$, CF_2Cl_2, CCl_4 and CH_3CCl_3. The atmospheric release (expressed in Tons/years) corresponding to an uniform vertical flux around the Earth (expressed in $cm^{-2}\ s^{-1}$) is given by the following numbers

Species	Total Emission (Tons/yr)	Flux ($cm^{-2}\ s^{-1}$)
CCl_4	1.0×10^5	2.46×10^6
$CFCl_3$	3.4×10^5	9.27×10^6
CF_2Cl_2	4.1×10^5	1.27×10^7
CH_3CCl_3	3.6×10^5	1.00×10^7

When present-day conditions are simulated, an observed mixing ratio is prescribed at the ground, namely

CCl_4	1.5×10^{-10}
$CFCl_3$	1.6×10^{-10}
CF_2Cl_2	2.8×10^{-10}
CH_3CCl_3	6.0×10^{-11}

Fig. 23 shows the mixing ratio and fig. 24 the vertical flux of the five most important halocarbons corresponding to the perturbed conditions (steady state values). Except for methylchloride which is destroyed by hydroxyl radicals in the troposphere, the flux of the verious halocarbons is almost constant up to 15 km since the destruction of these molecules appears only in the stratosphere. The most abundant man-made halocarbon when steady state is reached, appears to be CF_2Cl_2. It can also be seen that the amount of CCl_4 is quite unchanged from present day conditions.

The production of odd chlorine is depicted in fig. 25 for three different cases : natural atmosphere (only the CH_3Cl effect); present day atmosphere and perturbed atmosphere (steady state). The modification of the distributions, due to the industrial activity, appears essentially above 15 km, where the photodissociation happens. The maximum artificial production takes place around 25-30 km. In this region the value of the production is increased by a factor of 6 from natural to perturbed (steady state) conditions and of about 5 from present time to steady state. Fig. 26 shows the individual contribution of each important chlorocarbon to the production of total odd chlorine in the perturbed case. Finally, the vertical distribution of ClX and ClO for the three different conditions is represented in fig. 27. The relative density of chlorine atoms (mainly in the form of HCl) is respectively equal to 7.1×10^{-10}, 2.4×10^{-9} and 1.1×10^{-8} when the standard K profile is used.

The effect of a man-made production of odd chlorine on the ozonosphere appears through an increase in the loss rate of O_3 and consequently a decrease of the ozone concentration. However this effect is counterbalanced by the enhancement of the UV penetration at lower level and consequently by an increase in the O_3 production rate. This feedback mechanism introduces non linearities and the value of the new equilibrium can only be obtained by a detailed calculation. Fig. 28 represents the relative variation of the ozone concentration between

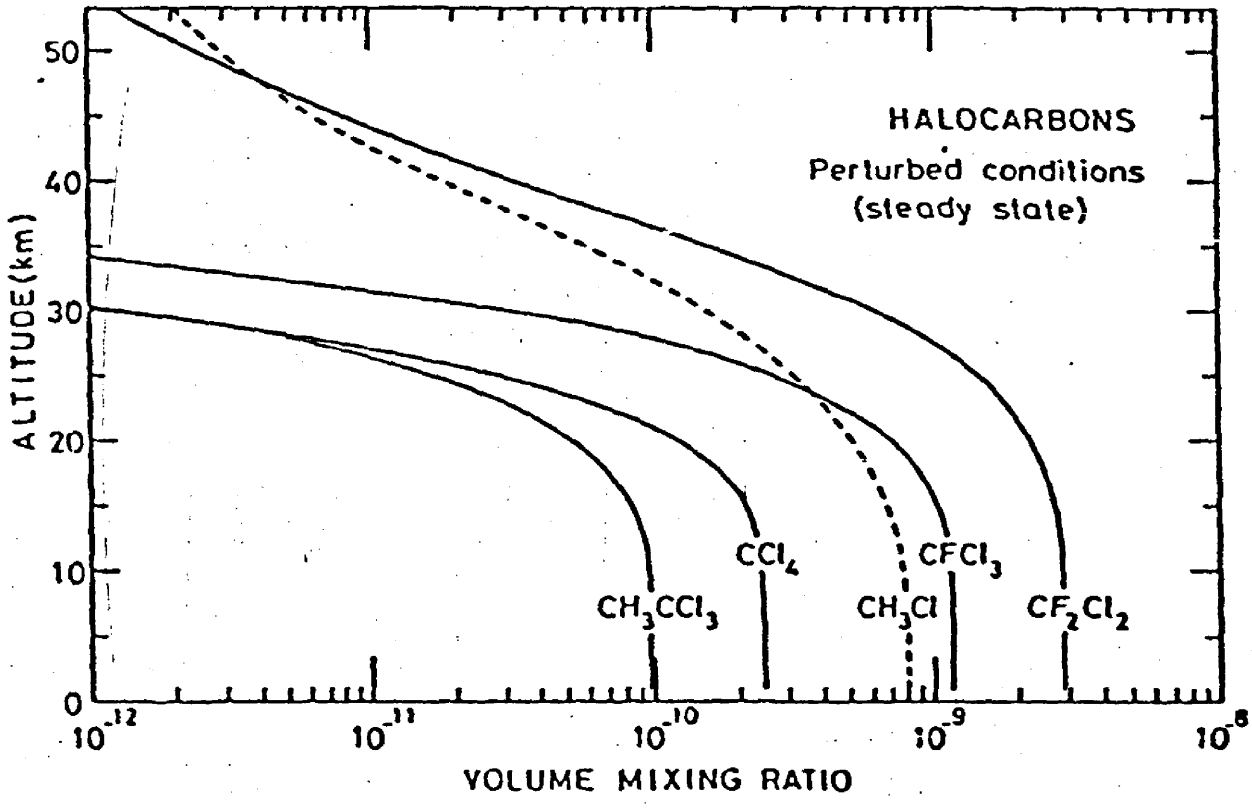

Fig. 23.- Mixing ratio of the most important halocarbons in relation with the ozone problem. Vertical distributions obtained in the steady state for perturbed conditions.

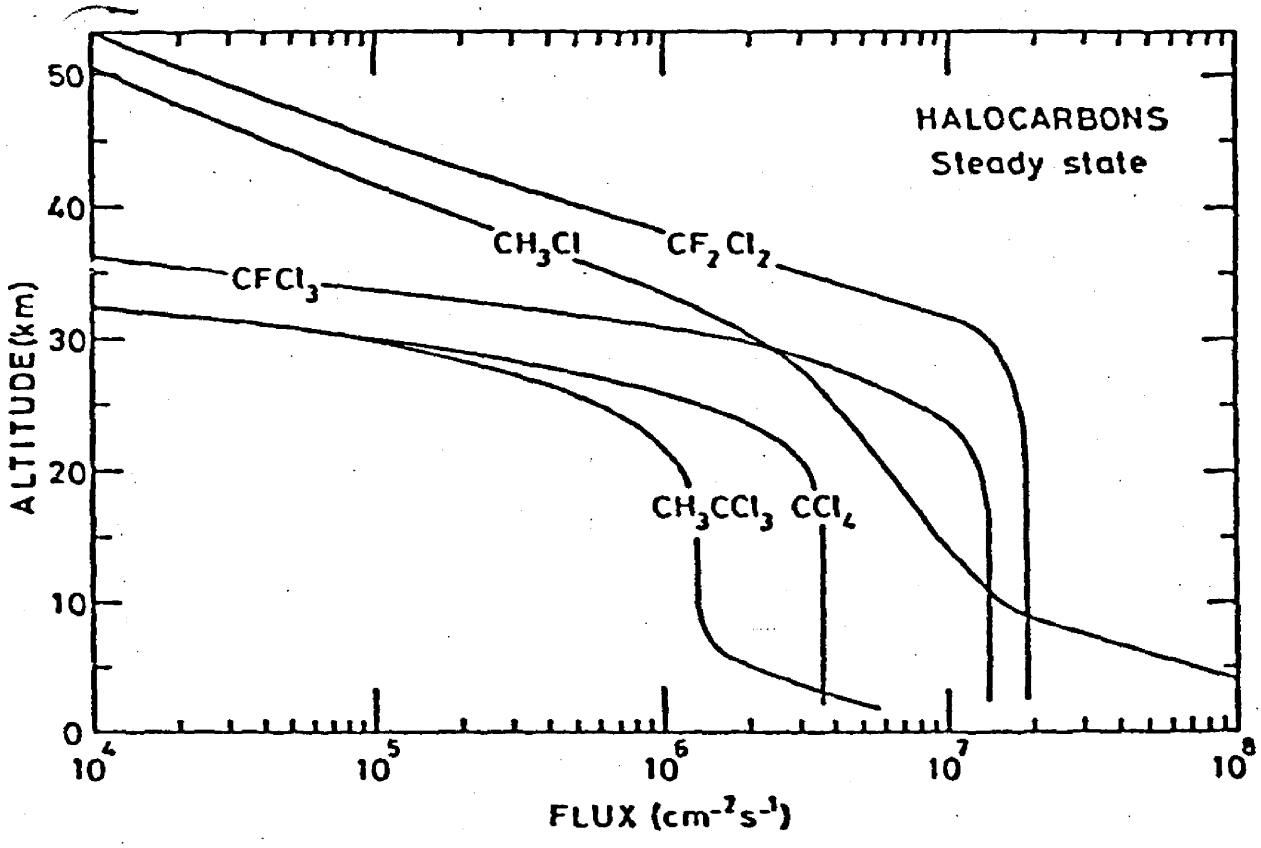

Fig. 24.- Same as 3.15 but vertical flux. The decrease appearing for CH_3Cl and CH_3CCl_3 is due to the tropospheric destruction by the hydroxyl radical.

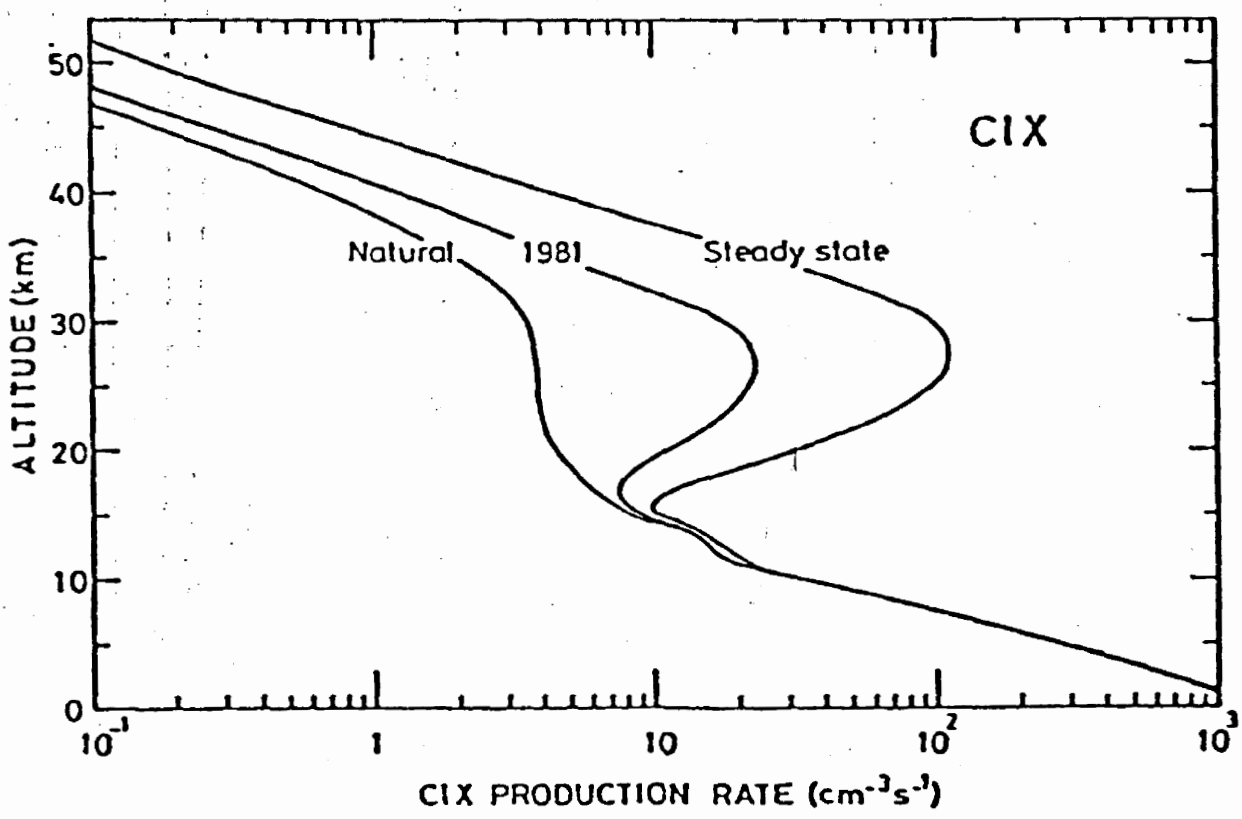

Fig. 25.- Vertical distribution of the odd chlorine production rate for three different cases : Natural atmosphere; present day atmosphere and perturbed conditions (steady state values).

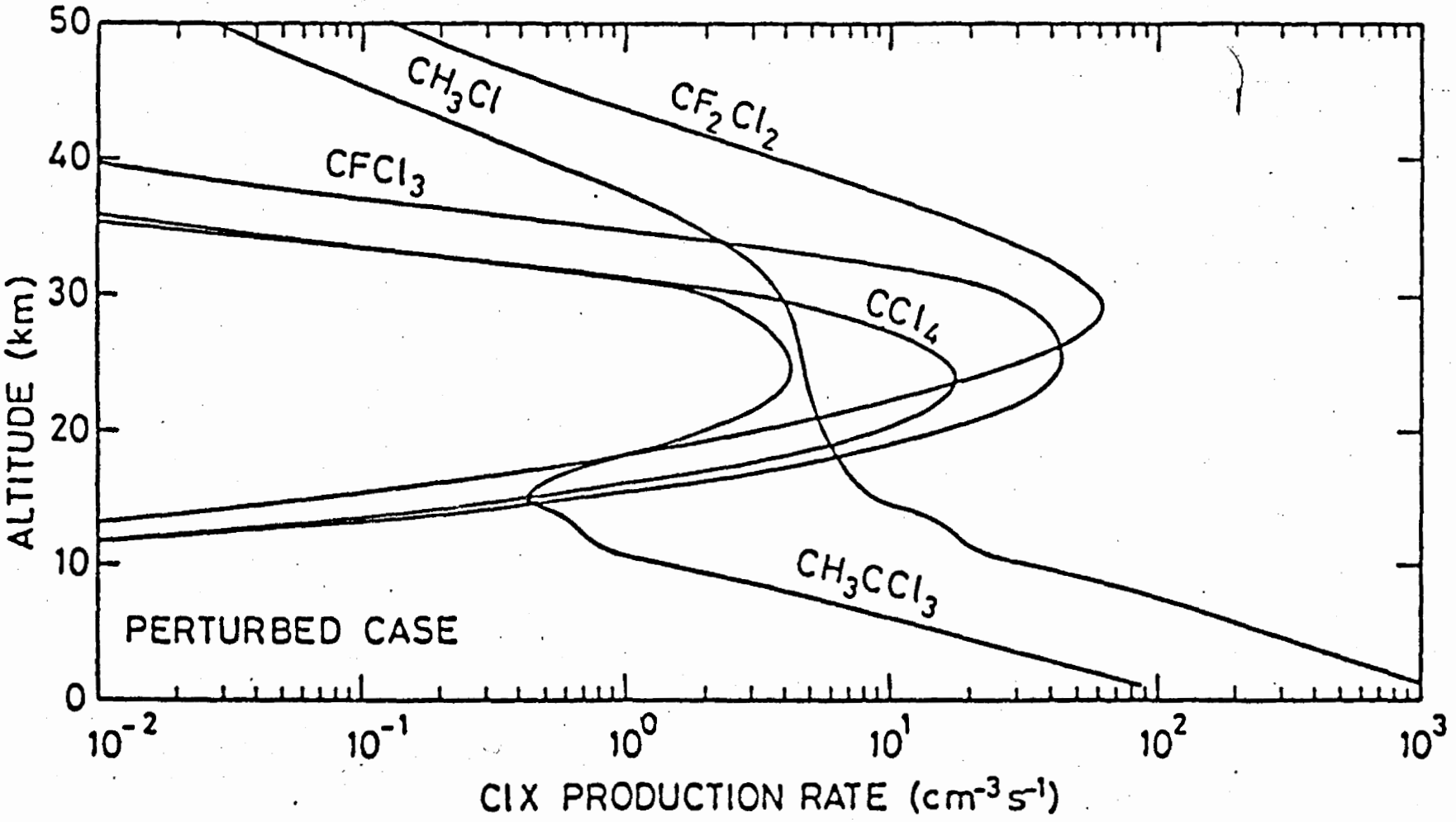

006

Fig. 26.- Effect of the different halocarbons in the odd chlorine production rate. Perturbed case (steady state values).

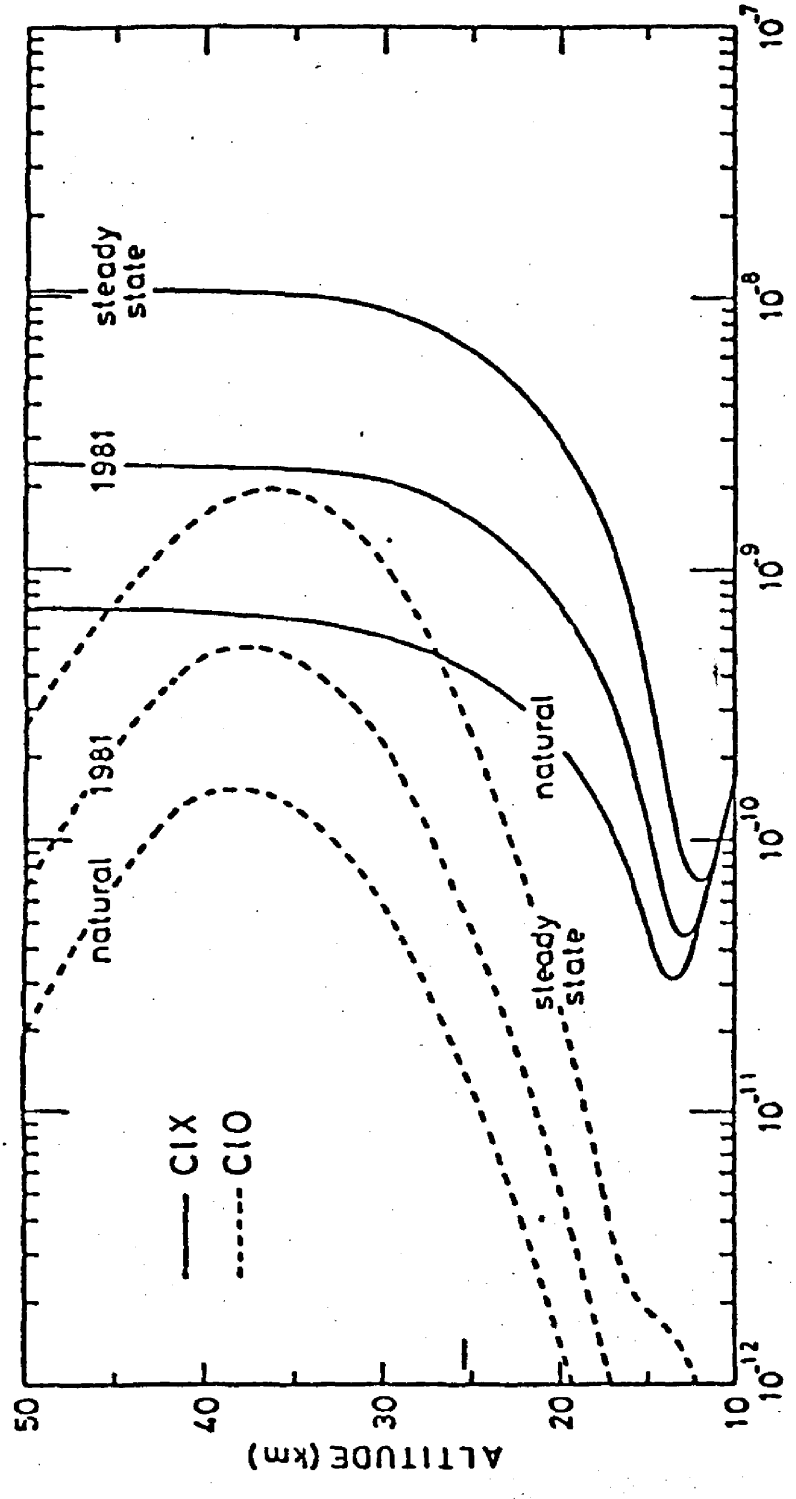

Fig. 27.- Vertical distribution of the ClX and ClO mixing ratio. Calculations performed in the three different cases : natural atmosphere, present day atmosphere, perturbed atmosphere (steady state values).

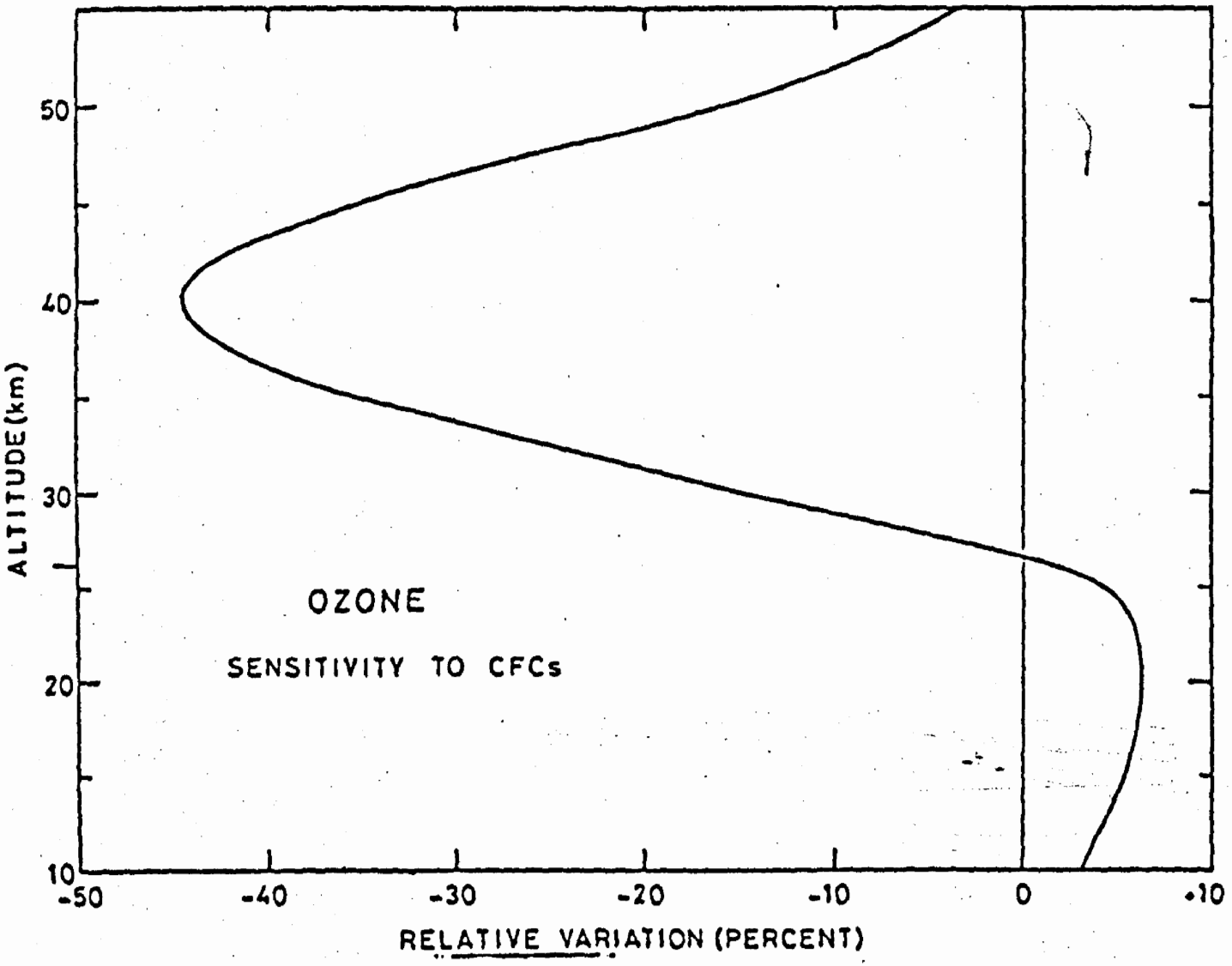

Fig. 28.- Vertical distribution of the relative ozone depletion due to a "standard" injection of chlorofluorocarbons (see text for emission rates). Steady state values.

perturbed conditions (steady state) and purely natural conditions. The maximum reduction appears around 40 km.

In the upper stratosphere, the ozone reduction is due essentially to the direct cycle .

$$\begin{aligned} Cl + O_3 &\longrightarrow ClO + O_2 \\ ClO + O &\longrightarrow Cl + O_2 \\ \hline \text{net } O + O_3 &\longrightarrow 2O_2 \end{aligned}$$

But, below 30 km, there is a displacement of Cl and ClO toward other chlorinated species such as HOCl and $ClONO_2$, with a corresponding lower efficiency of the direct catalytical cycle. However, species such as HOCl and $ClONO_2$ can induce supplementary cycles of ozone destruction, namely

$$\begin{aligned} Cl + O_3 &\rightarrow ClO + O_2 \\ ClO + HO_2 &\rightarrow HOCl + O_2 \\ HOCl + h\nu &\rightarrow Cl + OH \\ OH + O_3 &\rightarrow HO_2 + O_2 \\ \hline \text{net } 2O_3 &\rightarrow 3O_2 \end{aligned}$$

or

$$\begin{aligned} ClO + NO_2 &\rightarrow ClONO_2 \\ ClONO_2 + h\nu &\rightarrow Cl + NO_3 \\ Cl + O_3 &\rightarrow ClO + O_2 \\ NO_3 + h\nu &\rightarrow NO + O_2 \\ NO + O_3 &\rightarrow NO_2 + O_2 \\ \hline \text{net } 2O_2 &\rightarrow 3O_2 \end{aligned}$$

These cycles show the importance of the coupling between the different chemical families. Therefore, it is clear that the ozone reduction by ClX, especially in the lower stratosphere, depends on the behavior and concentration of species such as NO, OH, HO_2,...

The following table summarizes our model results which have been discussed when the effect of the diurnal variation is not included in the program (early model calculations) and for the "standard K".

Total ozone variation $\Delta O_3/O_3$	- 4.9%
Ozone variation at 40 km	- 51%
20 km	7.84%
Increase of ClX at the stratopause ΔCl_X (ppbv)	9.76

When the effect of the diurnal variation is introduced, the total ozone reduction is enhanced from 5 to 6 percent.

The sensitivity of the ozone depletion to the eddy diffusion profile has also been considered. All previous calculations in this section refer to the so-called "standard exchange coefficient". Similar model runs have been made with a K profile uniformly divided by 3 and with the distribution recently suggested by Massie and Hunten (1981). The following table gives the corresponding results

Variation in the	K(stand)	K/2	K/3	K(Massie)
ozone column $\Delta O_3/O_3$ (%)	- 6.1	- 7.3	- 9.1	- 10.3
Ozone variation (%) at				
40 km	- 53.3	- 72.9	- 81.7	- 76.6
20 km	+ 8.5	+ 17.5	+ 20.7	+ 19.0

Total chlorine at					
50 km	nat.	0.71	0.62	0.55	0.71
(ppbv)	perturb.	10.49	15.94	20.30	21.77
Increase of the ClX mixing ratio at the stratopause					
ΔCl_X (ppbv)		9.78	15.32	19.75	21.06
$\Delta O_3/O_3$ (%)/ΔClX (ppbv)		- 0.62	- 0.48	- 0.46	- 0.49
$\Delta O_3/O_3$ at 40 km/ΔClX (ppbv)		- 5.45	- 4.76	- 4.13	- 3.64
Total chlorine at ground level (perturb.) (ppbv)		10.9	17.3	22.5	22.5

4.2. Potential changes due to other perturbations

Nitrous oxide is the principal source of nitric oxide. Its production at ground level will be enhanced if the use of fertilizers becomes more and more intensive. In order to analyze the possible effect of such a continuous emission of N_2O in the atmosphere, a conventional perturbation is applied in the mathematical model : the concentration of N_2O is uniformly doubled and the impact of such a modification is estimated. In fact, the model shows a decrease of the ozone amount particularly between 20 and 40 km. Simultaneous perturbations can also be simulated, namely a doubling of N_2O and a CFC standard release. The results, which are obtained, are given in the following table (no diurnal variation effect) :

	$2 \times N_2O$	CFC	$2 \times N_2O$ + CFC
ΔO_3 (%)	- 10.7	- 4.9	- 12.4

This table shows the non linear response of the two simultaneous perturbations. In fact, if one of the two effects is clearly dominant,

the second perturbations does not modify considerably the total ozone depletion.

The impact of aircraft operations has also been studied. Different flying altitudes have been considered with two specific NO_x injection rates. The results are given in the following table

Injection altitude (km)	NO_x injection rate ($cm^{-2}\ s^{-1}$)	Ozone variation (%)
13	2×10^8	- 0.7
17	1×10^8	- 1.8
	2×10^8	- 2.7
20	1×10^8	- 3.6
	2×10^8	- 6.4

The injection of 1×10^8 cm^{-2} s^{-1} represents about 300 Concorde flying each day and corresponds to more or less the value of the natural production of NO_x in the stratosphere.

ACKNOWLEDGMENTS

This work has been supported by the Chemical Manufacturers Association (CMA) under contract n° 80-320.

REFERENCES

ACKERMAN, M., J.C. FONTANELLA, D. FRIMOUT, A. GIRARD, N. LOUISNARD and C. MULLER, Planet. Space Sci., 23, 651-660, 1975.

ACKERMAN, M., D. FRIMOUT, C. MULLER and D.J. WUEBBLES, Pageoph, 117, 367-380, 1978.

ANDERSON, J.G., H.J. GRASSL, R.E. SHETTER and J.J. MARGITAN, Stratospheric free chlorine measured by balloon borne in situ resonance fluorescence, Manuscript dated February 1979.

ANDERSON, J.G., in Proceedings of the NATO Advanced Study Institute on Atmospheric Ozone, (Portugal) edited from the U.S. Dept. of Transportation, FAA-Washington, D.C., USA, Report n° FAA-80-20, 1980.

BATES, J.R. and M. NICOLET, J. Geophys. Res., 55, 301, 1950b.

BAUER, E. and F.R. GILMORE, Rev. Geophys. Space Phys., 13, 451-458, 1975.

BLOXAM, R.M., A.W. BREWER and C.T. McELROY, Proceedings of the Fourth CIAP Conf. US Dept. Transportation, DOT-TSC-OST-75-38, 454, 1975.

BRASSEUR, G., Planet. Space Sci., 26, 139, 1978.

BRASSEUR, G., Proceedings of the NATO Advances Study Institute on Atmospheric Ozone, Albufeiras, Portugal, (A. Aikin, ed), 1980.

BRASSEUR, G., Physique et Chimie de l'Atmosphère Moyenne, Masson, Paris, 1982.

BRASSEUR, G. and M. NICOLET, Planet. Space Sci., 21, 939, 1973.

BRASSEUR, G. and P.C. SIMON, J. Geophys. Res., 86, 7343-7362, 1981.

CESS, R.D. and V. RAMANATHAN, J. Quant. Spectrosc. Radiat. Trans., 12, 933, 1972.

CHAPMAN, S., Memoir. Roy. Met. Soc. London, 103, 1930.

CRUTZEN, P.J., Quart. J. Roy. Meteorl. Soc., 96, 320, 1970.

CRUTZEN, P.J., Ambio, 1, 41, 1972.

CRUTZEN, P.J., Tellus, 26, 47, 1974.

CRUTZEN, P.J., Geophys. Res. Lett., 3, 73-76, 1976.

CRUTZEN, P.J. et al., Science, 189, 457-458, 1975.

DEMAZURE, M. and J. SAISSAC, Généralisation de l'équation classique de diffusion, Note de l'Etablissement d'Etudes et de Recherches Météorologiques n°115, Paris, 1962.

DRUMMOND, J.R. and R.F. JARNOT, Proc. Roy. London, Ser. A, 364, 237-254, 1978.

DRUMMOND, J.R., J.M. ROSEN and D.J. HOFMANN, Nature, 265, 319-320, 1977.

EDWARDS, D.K., Appl. Optics, 4, 1278, 1965.

EHHALT, D.H., L.E. HEIDT, R.M. LUEB and N. ROPER, in Proceedings of the "Third Conference on CIAP", Febr. 1974, U.S. Department of Transportation, p. 153-160, 1974.

EVANS, W.F.J., J.B. KERR, D.I. WARDLE, J.C. McCONNEL, B.A. RIDLEY and H.I. SCHIFF, Atmosphere, 14, 189-198, 1976.

FABIAN, P., R. BORCHERS, K.H. WEILER, U. SCHMIDT, A. VOLZ, D.H. EHHALT, W. SEILER and F. MULLER, J. Geophys. Res., 84, 3149-3154, 1979.

FARMER, C.B., O.F. RAPER, B.D. ROBBINS, R.A. ROTH and C. MULLER, J. Geophys. Res., 85, 1621-1632, 1980.

FOLEY, H.M. and M.A. RUDERMAN, Pap. P-984, Inst. for Def. Anal., Arlington, Va., 1972.

FOLEY, H.M. and M.A. RUDERMAN, J. Geophys. Res., 78, 4441-4450, 1973.

FONTANELLA, J.-C., A. GIRARD, L. GRAMONT and N. LOUISNARD, in Proceedings of the Third CIAP Conference, DOT-TSC-OST-74-15, p. 217, U.S. Dept. of Transp., Washington, D.C., 1974 and Applied Optics, 14, 825, 1975.

FREDERICK, J.E. and R.D. HUDSON, J. Molec. Spec., 74, 247-258, 1979.

GOLDAN, P.D., W.C. KUSTER, D.L. ALBRITTON and A.L. SCHMELTEKOPF, J. Geophys. Res., 85, 413-423, 1980.

GOLDSMITH, P.A., A.F. TUCK, J.S. FOOT, E.L. SIMMONS and R.L. NEWSON, Nature, 244, 545-551, 1973.

HARRIES, J.E., Nature, 274, 235-236, 1978.

HARRIES, J.E., D.G. MOSS, N.R.W. SWANN, G.F. NEILL and P. GILDWARD, Nature, 259, 300-301, 1976.

HERING, W.S. and T.R. BORDEN, Ozone sonde observations over North America, vol. 3, AFCRL-64-30 (III), Air Force Cambridge, Research Labs., Bedford, Mass, 1965.

HORVATH, J.J. and G.J. MASON, Geophys. Res. Lett., 5, 1023-1026, 1978.

JARNOT, R.F., Radiometric measurements of atmospheric minor constituents, D. Phil. Thesis, Oxford University, 1976.

JOHNSTON, H.S., Science, 173, 517, 1971.

JOHNSTON, H., G. WHITTEN and J. BIRKS, J. Geophys. Res., 78, 6107, 1973.

KOCKARTS, G., Planet. Space Sci., 24, 589, 1976.

KRUEGER, A.J. and R.A. MINZNER, J. Geophys. Res., 81, 4477, 1976.

LOEWENSTEIN, M., W.L. STARR and D.G. MURCRAY, Geophys. Res. Lett., 5, 531-535, 1978.

LOGAN, J.A., M.J. PRATHER, S.C. WOFSY and M.B. McELROY, Phil. Trans. Roy. Soc. London, 290, 187-234, 1978.

MAIER, E.J., A.C. AIKIN and J.E. AINSWORTH, Geophys. Res. Lett., 5, 37-40, 1978.

MASON, C.J. and J.J. HORVATH, Geophys. Res. Lett., 3, 391-394, 1976.

MASSIE, S.T. and D.M. HUNTEN, J. Geophys. Res., 86, 9859, 1981.

McELROY, M.B., J.W. ELKINS, S.C. WOFSY and Y.L. YUNG, Rev. Geophys. Sp. Phys., 14, 143-150, 1976.

MENZIES, R.T., Geophys. Res. Lett., 6, 151, 1979.

MOLINA, J.S. and F.S. ROWLAND, Nature, 249, 810, 1974a.

MOLINA, J.S. and F.S. ROWLAND, Geophys. Res. Lett., 1, 309, 1974b.

MURCRAY, D.G. et al., Résultats présentés à l'Assemblée de l'IAMAP, Melbourne, Australie, 1974.

NICOLET, M., Canad. J. Chem., 52, 1381, 1974.

NICOLET, M., Rev. Geophys. and Space Phys., 13, 593, 1975.

NICOLET, M., Planet. Space Sci., 23, 637, 1975.

NICOLET, M. and W. PEETERMANS, Planet. Space Sci., 28, 85, 1980.

PARRISH, A., R.L. de ZAFRA, P.M. SOLOMON, J.W. BARRETT and E.R. CARLSON, Science, 211, 1158-1161, 1981.

PENKETT, S.A., K.A. BRICE, R.G. DERWENT and A.E.J. EGGLETON, Atmos. Environ., 13, 1011-1019, 1979.

RAMANATHAN, V., Second International Conference on the Environmental Impact of Aerospace Operations in the High Atmosphere, July 8-10, 1974, San Diego, California, American Meteorological Society, Boston, Ma, USA.

RAMANATHAN, V., J. Atmos. Sci., 33, 1330-1346, 1976.

REED, R.J. and K.E. GERMAN, Month. Weather Rev., 93, 313, 1965.

RIDLEY, B.A., H.I. SCHIFF, A. SHAW and J.R. MEGILL, J. Geophys. Res., 80, 1925-1929, 1975.

RIDLEY, B.A., J.T. BRUIN, H.I. SCHIFF and J.C. McCONNELL, Atmosphere, 14, 180-188, 1976.

SCHMIDT, U., J. RUDOLPH, F.J. JOHNEN, D.H. EHHALT, A. VOLZ and E.P. ROTH, Proc. Quadriennal International Ozone Symposium, Boulder, Colorado, 4-9 August, 1980.

SCHOEBERL, M.R. and D.F. STROBEL, J. Atmos. Sci., 35, 577, 1978.

STOLARSKI, R.S. and R.J. CICERONE, Can. J. Chem., 52, 1610, 1974.

TRENBERTH, K.E., Monthly Weather Review, 101, 4, 287-305, 1973.

W.M.O., The stratosphere 1981, Theory and Measurements, W.M.O., Case Postale n°5, Geneva 20, Switzerland, 1982.

ZANDER, R., H. LECLERCQ and L.D. KAPLAN, Geophys. Res. Lett., 8, 4, 365-368, 1981.